GEAR TECHNOLOGY

The Journal of Gear Manufacturing

JULY/AUGUST 1986

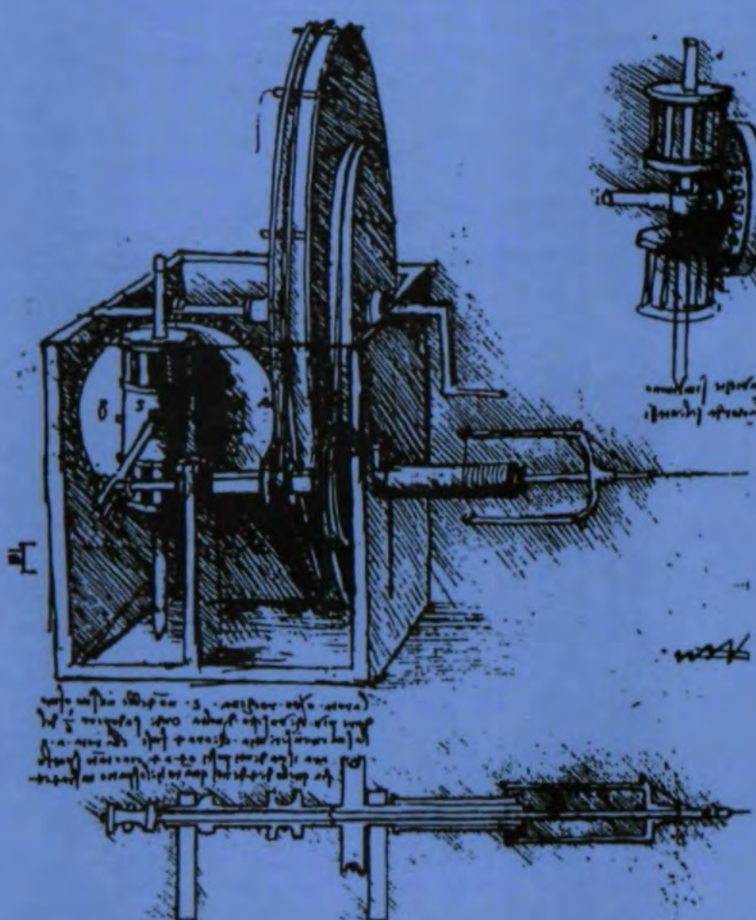

Mechanical Efficiency of Differential Gearing

Effect of MoS_2 Films on Scoring Resistance of Gears

Engineering Constants

Bevel Gear Development and Testing Procedure




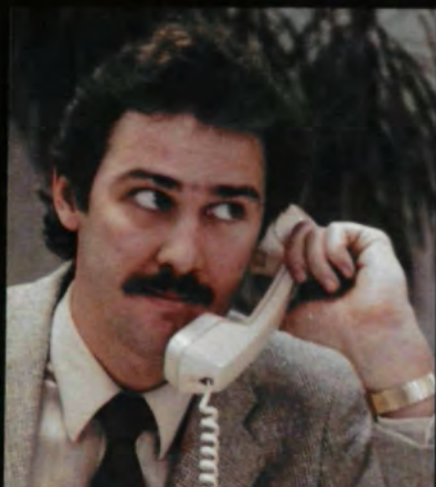

PFAUTER PE150
PFAUTER






GEAR TECHNOLOGY

The Journal of Gear Manufacturing

RANDALL PUBLISHING
1401 Lunt Avenue
P.O. Box 1426
Elk Grove, IL 60007
(312) 437-6604

TYPOGRAPHY:
Kenric Graphics, Inc.
Elk Grove Village, IL

PRINTING:
TCR Graphics
Streamwood, IL

The Advanced Technology of Leonardo Da Vinci 1452-1519

COVER

In his own lifetime, Leonardo was known as much for his engineering projects as for his painting. Every official appointment he received refers to him as both "engineer and painter."

The cover sketch is another of Leonardo's studies for textile machinery. It shows an automated spool-winding machine. The crank turns the bobbin and the flyer, the wishbone-shaped mechanism, in opposite directions. At the same time, the gear mechanism, shown in detail at the top of the sketch, moves it back and forth to insure even distribution of the thread on the bobbin.

CONTENTS — PAGE NO.

FEATURES

DEPARTMENTS

July/August 1986 — Vol. 3, No. 4

GEAR TECHNOLOGY, The Journal of Gear Manufacturing (ISSN 0743-6858) is published bimonthly by Randall Publishing Co., Inc., 1425 Lunt Avenue, P. O. Box 1426, Elk Grove Village, IL 60007. GEAR TECHNOLOGY, The Journal of Gear Manufacturing is distributed free of charge to qualified individuals and firms in the gear manufacturing industry. Subscription rates for non-qualified individuals and firms are: $30.00 in the United States, $50.00 for foreign countries. Second-Class postage paid at Arlington Heights, IL and at additional mailing office.

Postmaster: Send address changes to GEAR TECHNOLOGY, The Journal of Gear Manufacturing, 1425 Lunt Avenue, P. O. Box 1426, Elk Grove Village, IL 60007.

MANUSCRIPTS: We are requesting technical papers of every sort from manufacturers of gear making machinery and related equipment, universities, and engineers. Articles should be of an educational and training nature with general appeal to anyone having anything to do with the purchase of materials or machinery, or the design, manufacture, testing or processing of gears. Subjects sought are solutions to specific problems, explanations of new: technology, techniques, designs, processes, and alternative manufacturing methods. These can range from the "How to . . ." of gear cutting (BACK TO BASICS) to the most advanced technology. All manuscripts submitted will be carefully considered. However, the Publisher assumes no responsibility for the safety or return of manuscripts. Manuscripts must be accompanied by a self-addressed, self-stamped envelope, and be sent to GEAR TECHNOLOGY, The Journal of Gear Manufacturing, P.O. Box 1426, Elk Grove, IL 60007, (312) 437-6604.

ADVERTISER'S INDEX FOR IMTS

(In-house exhibition)
American Pfauter
925 E. Estes Ave.
Elk Grove, IL 60007
(312) 640-7500

Booth #2002
McCormick, East Level 2
Fette
Division of Saarberg Intertool Inc.
P.O. Box 9, 3650 N. 126th Street
Brookfield, WI 53005
(414) 783-7606

Booth 6243
McCormick North Level 2 (COSA)
Forest City Gear
11715 Main Street
Roscoe, IL 61073
(815) 623-2168

Booth 8818
McCormick Place West
Fromag GmbH
R. J. Kemp, Representative
38 W510 Lake Charlotte Ct.
St. Charles, IL 60174

Booth #4454
McCormick, East Level 3
GMW Machinery Inc.
Gear Machinery Division
1665 Tonne Avenue
Elk Grove Village, IL 60007
(312) 364-4530

Booth #3333
McCormick, North
The Gleason Works
1000 University Avenue
Rochester, NY 14692
(716) 473-1000

Booth #6097
McCormick, North
Hoglund Tri-Ordinate Corp.
343 Snyder Avenue
Berkeley Heights, NJ 07922
(201) 464-0200

Booth #2219
McCormick, East
ITW Illinois Tools
ITW Illitron
3601 W. Touhy Avenue
Lincolnwood, IL 60645
(312) 761-2100

Booth #5009
McCormick, North
Klingelnberg Corporation
15200 Foltz Industrial Parkway
Strongsville, OH 44136
(216) 572-2100

Booth #5252
McCormick, North
Liebherr Machine Tool
290 South Wagner Rd.
Ann Arbor, MI 48103
(313) 769-3521

Booth #6281
McCormick, North
Mitsubishi Heavy Industries America, Inc.
873 Supreme Drive
Bensenville, IL 60106
(312) 860-4220

Booth #6279
McCormick, North
Perez Machine Tool Co.
11 Ginger Court
East Amherst, NY 14051
(716) 688-6982

Booth #6343
McCormick, North
StarCut Sales, Inc.
23461 Industrial Park Drive
Farmington Hills, MI 48024
(313) 474-8200

IMTS
The world of manufacturing technology

1986 INTERNATIONAL MACHINE TOOL SHOW
September 3-11, 1986 • Chicago, Illinois, USA

VIEWPOINT

"VIEWPOINT" provides an opportunity for readers to discuss problems and questions facing our industry.

Please address your questions and answers to: VIEWPOINT, GEAR TECHNOLOGY, P.O. Box 1426, Elk Grove Village, IL 60007.

Dear Editor:

Since we are a high volume shop, we were particularly interested in Mr. Kotlyar's article describing the effects of hob length on production efficiency which appeared in the Sept/Oct issue of GEAR TECHNOLOGY. Unfortunately, some readers may be unnecessarily deterred from applying the analysis to their own situations by the formidability of the mathematical calculations. I am making the following small suggestion concerning the evaluation of the constant terms.

The article's author adroitly recognizes that the ratio $a/b = \sin(q)$ when he uses equation (2.3) of the line in reducing the three equations into one polynominal in order to determine the length of the roughing zone. That same relationship can be employed in equation (2.2) of the workpiece eclipse; that is:

$$X^2 = (a/b)^2 (b^2 - Y^2) = (b^2 - Y^2)\sin^2 q$$

When the substitution for X^2 is made by using the above equality, the original constants of the fourth degree polynominal are reduced to simple single term expressions in four of the five terms:

$$KA = \cos^2 q$$

$$KB = -2Y_0 \cos^2 q$$

$$KC = Y_o^2 \cos^2 q + (HD/2)^2 \sin^2 q - b^2$$

$$KD = +2b^2 Y_o$$

$$KE = -b^2 Y_o^2$$

R. Mory
Process Engineer
Gear Development Department
Ford Motor Trans. & Chassis Div.
Livonia, Michigan

(continued on page 43)

NOTES FROM THE EDITOR'S DESK

The last two months have been both a time of difficulty and of growth for GEAR TECHNOLOGY. Unexpectedly, I found myself in the hospital, having surgery, and consequently out of commission for several weeks. At the same time, two individuals on our staff lost family members, and most of this period saw us getting ready for this preshow IMTS issue while being seriously short-staffed.

Problems, however, can often be turned into opportunities. We saw how well everyone pulled together to get the job done, each person extending themselves for others. G.T. has since added two new staff members, and we are now looking forward to continued growth in our work and in our industry.

September 3-11, 1986, the International Machine Tool Show will be held at McCormick Place Exposition Center. This show will be even larger than in years past, expanding to occupy over 2 million square feet. We will see a much needed improvement, a change of organization of exhibitors that will place manufacturers of similar lines in one area. Most Gear Equipment Manufacturers will be located in the new McCormick Place North. This should make your visit to the show easier and more productive.

As an added convenience to our readers, we have included a special index of our advertisers with *booth numbers and building locations. This index* will help you find the equipment you have been reading about. A preliminary index will appear in this issue, and next issue. Make your travel arrangements to Chicago early — this could be the biggest show yet.

Michael Goldstein
Editor/Publisher

IMTS 1986
"THE WORLD OF MANUFACTURING TECHNOLOGY"

McCormick Place North will expand IMTS-86 exhibit space to 1 million sq. ft. Houses registration & conference areas. Most Gear manufacturers will be in this building.

September 3-11 the 1986 International Machine Tool Show, "The World of Manufacturing Technology", will be held at the McCormick Place Exposition Center in Chicago. More than 1000 exhibits from over thirty countries are planned. These exhibits will present a complete range of machine-tool products from 2-story high presses to complete manufacturing systems, lathes, lasers, CAD/CAM systems and robotics.

This year's show will have a number of improvements over previous exhibitions. For the first time, the entire exposition will be all in one place. All three buildings of the McCormick Place complex, including the new North Annex, will be used for the show. Similar product lines will be grouped together to enable visitors to more easily locate the types of products which are of interest to them.

In conjunction with the show itself, the Third Biennial International Machine Tool Technical Conference will be held. This conference will feature more than 300 papers on over 100 subjects.

The show, which will be open from 9:00 am through 6:00 pm, is located just south of the Chicago loop and is easily accessible by both automobile and public transportation. This location puts visitors near hotels, restaurants, shopping, and major museums. Many hotels and restaurants, are also located near O'Hare Airport. Visitors arriving at O'Hare Airport will find public transportation easily available. Those traveling by car can access the Kennedy Expressway which runs directly between O'Hare and the exposition center on Lake Shore Dr. For more information on hotels, entertainment and transportation in Chicago, contact the Chicago Convention and Tourism Bureau, (312) 225-5000 or the Illinois Office of Tourism, (800) 223-0121.

For copies of registration forms or for more information on IMTS call (301) 662-9412. Individuals registering before August 3, 1986 will receive a 50% discount.

Before you buy a CNC Gear Inspection System, ask these four questions

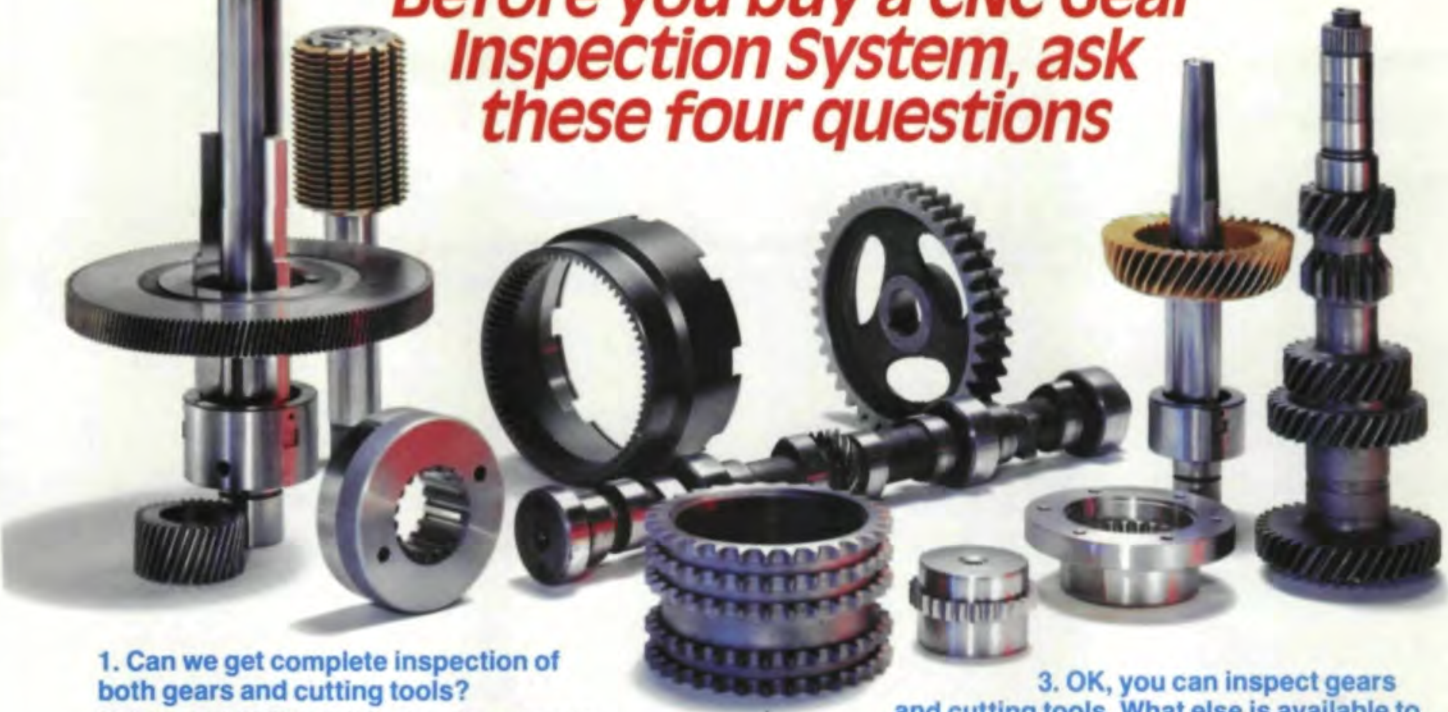

1. Can we get complete inspection of both gears and cutting tools?

With the M & M 2000 QC System, the answer is yes. The system will test lead and involute profile characteristics of internal or external gears and splines. It is the only universal gear tester available which provides true index testing without expensive attachments. In addition, we have fully-developed software for checking hobs, shaver cutters, shaper cutters, and other cylindrical parts such as worms and cams.

Hob Pressure Angle Check

Shaver Cutter Lead Check

2. Can you customize software to meet our quality-inspection specifications?

At M & M Precision, we write and develop our own inspection software. Our technical team can and has implemented inspection specifications into specific software for individual requirements. Our current library includes line/curve fitting as well as modified K-chart analysis routines.

Line/Curve Fitting

Modified K-Chart Analysis

3. OK, you can inspect gears and cutting tools. What else is available to aid us in quality control of the manufacturing process?

At M & M Precision, we have fully integrated such advanced software packages as Statistical Process Control and Tooth Topography into our standard testing software. Our SPC program can identify non-random variations and provide early warning of variations which are approaching tolerance limits. Our Tooth Topography software features automatic testing of lead and involute at multiple locations and provides two- and three-dimensional graphics.

SPC Run Chart

Topological Map

4. Do you have the technical support team and installation experience to back up the hardware and software provided?

At M & M Precision, we have a technical team with over 45 man-years of experience in developing CNC gear inspection hardware and software. All software for our QC 2000 System has been developed in-house. In addition, we have working installations at these leading companies:

- General Motors
- TRW
- Ford Motor
- Warner Gear
- Cincinnati Milacron
- Chrysler
- Pratt & Whitney
- Rocketdyne

For details on our advanced QC 2000 System and available software, contact M & M Precision Systems, 300 Progress Road, West Carrollton, Ohio 45449, 513/859-8273.

M&M PRECISION SYSTEMS

AN ACME CLEVELAND COMPANY

CIRCLE A-6 ON READER REPLY CARD

Mechanical Efficiency of Differential Gearing

D. Yu
N. Beachley
University of Wisconsin
Madison, Wisconsin

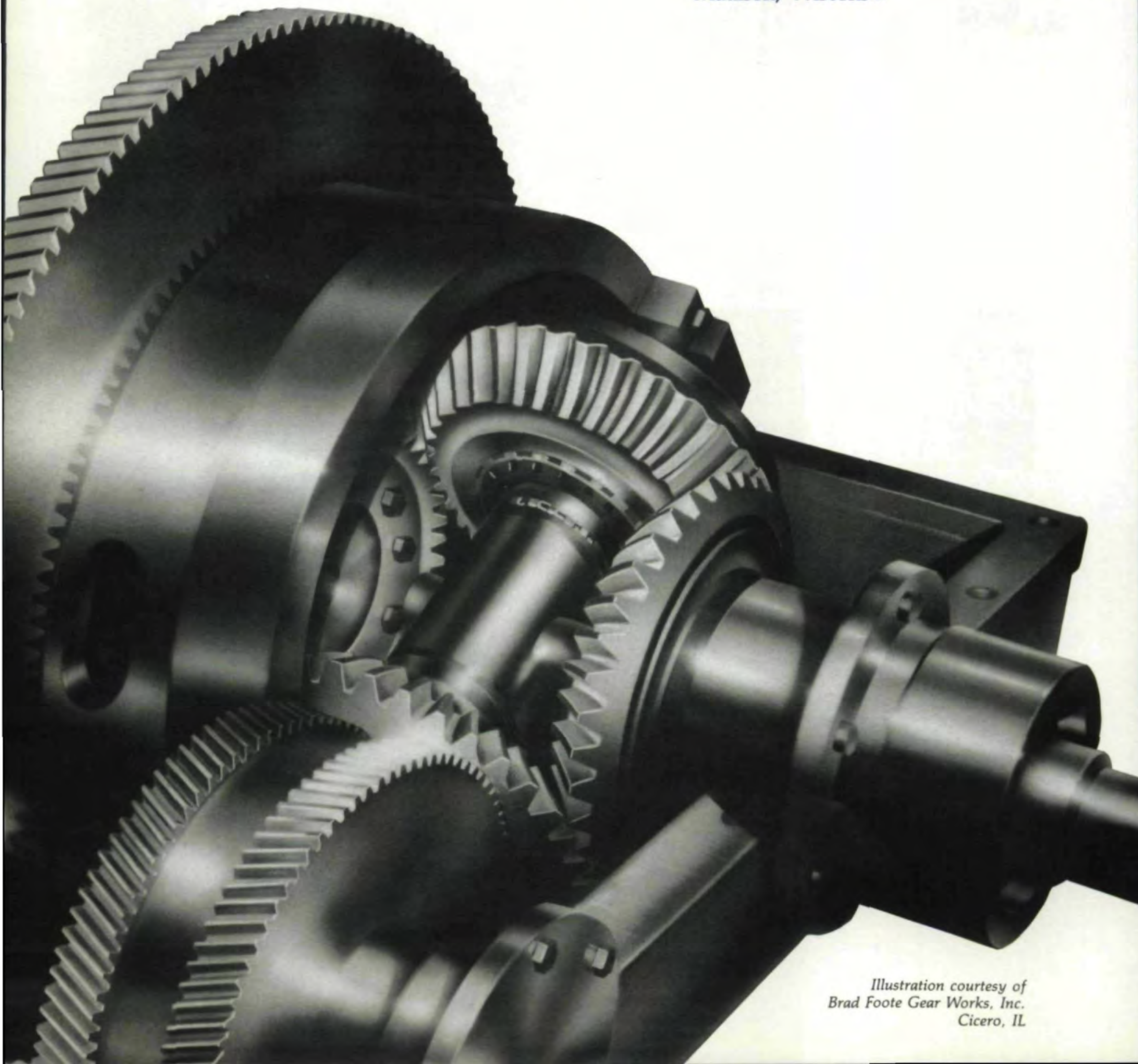

Illustration courtesy of Brad Foote Gear Works, Inc. Cicero, IL

Introduction

Mechanical efficiency is an important index of gearing, especially for epicyclic gearing. Because of its compact size, light weight, the capability of a high speed ratio, and the ability to provide differential action, epicyclic gearing is very versatile, and its use is increasing. However, attention should be paid to efficiency not only to save energy, but sometimes also to make the transmission run smoothly or to avoid a self-locking condition. For example, a Continuously Variable Transmission (CVT) is attractive for motor vehicles (and especially for flywheel or other energy storage hybrid vehicles), but most types of CVT have poor efficiency, and the energy loss of a vehicular CVT can be comparable to the road load energy.[1] The split-path or bifurcated power transmission is one promising type of CVT, consisting in some cases of differential gearing and a traction drive used to change the speed ratio continuously (Fig. 1). It is convenient to call the latter a Continuously Variable Unit (CVU) to differentiate it from the overall CVT system. Traction drive systems have a significant loss through slip and creep; therefore, it is important to reduce the amount of power flowing through the CVU as much as possible; and many studies concerning this problem have been done.[2-6] In most of them, however, the efficiency of the differential has not been taken into account, consequently the calculated overall efficiencies will not match those of a real system, and in some cases may be quite different. It is not practical to use an average value of efficiency either, because unlike conventional gearing, the efficiency of differential gearing is very sensitive to changes in speed ratio.

A common method for calculating the efficiency of epicyclic gearing is the so-called "latent power" or "gearing power" method. Although the name of the method and the procedure of deriving the formulas are somewhat different in some articles, the derived formulas are similar.[7-11] In most articles, however, emphasis has not been given to the differential, which has more than one degree of freedom, but instead given to planetary gearing that has only one degree of freedom and is simpler to analyze. Therefore, it is important to develop an explicit and general method for calculating the efficiency of differential gearing.

AUTHORS:

DR. DAVID YU *is a Consulting Engineer for Reliance Electric Co. Since 1982 he has been an Honorary Fellow of the University of Wisconsin at Madison. In the academic arena, he has served as the Deputy Head of the Mechanical Engineering Department, and as Professor of Machine Design at a Chinese University. Professor Yu is the author of numerous articles on gearing. He is a member of CMES and JSME.*

DR. NORMAN BEACHLEY *teaches undergraduate courses in the mechanical design area and graduate level courses in fluid power and analysis and design of rotating machinery. He is coauthor of the textbook* Introduction to Dynamic System Analysis.

His current research includes microprocessor control of internal combustion engines/hydrostatic transmission systems. He is also investigating the efficiency characteristics of various types of split-path, continuously variable transmissions.

A new project is to study novel internal combustion engine designs with greatly reduced mechanical friction.

General Considerations and Definitions

It is necessary and important to provide some precise and accurate definitions, otherwise confusion and mistakes are liable to occur.

Fundamental Differential. A fundamental differential has three basic members that can input or output power, including the carrier (Fig. 2). Without a carrier, there is no differential, so the carrier is an important member and is symbolized as H. Strictly speaking, a fundamental differential has two degrees of freedom, i.e., two constraints must be given, otherwise the relationships among the three members are independent. For example, if two of the three members are given as inputs, then the other can be determined as the output. It is also possible to have one input and two outputs, and knowing any two values makes it possible to calculate the third. The fundamental differential is the most common one, and types with more than two degrees of freedom are seldom used; thus, in this article the study is restricted to the fundamental differential.

Speed Ratio. The angular speed ratio is defined as

$$r_{ab} = N_a / N_b$$

or

$$r_{ba} = N_b / N_a = 1 / r_{ab},$$

If $r_{ab} > 0$, then a and b have the same direction of rotation, and if $r_{ab} < 0$, then opposite directions. "Same direction" means both have positive (or both negative) rotation, where positive has in each case an arbitrarily defined sense. If $|r_{ab}| > 1$, then from a to b is a reduction, and if $|r_{ab}| <$

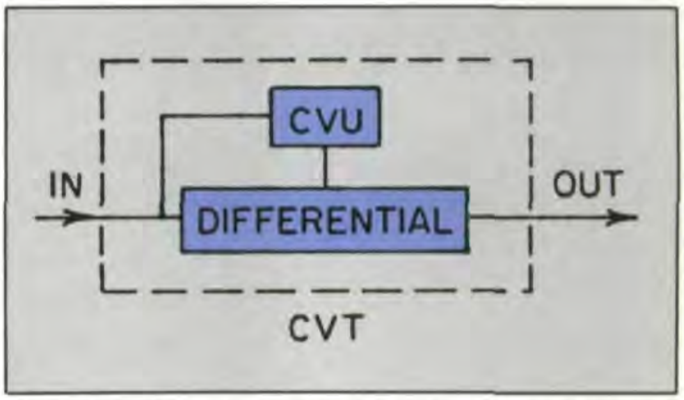

Fig. 1 – Schematic diagram of a split-path continuously-variable transmission (CVT)

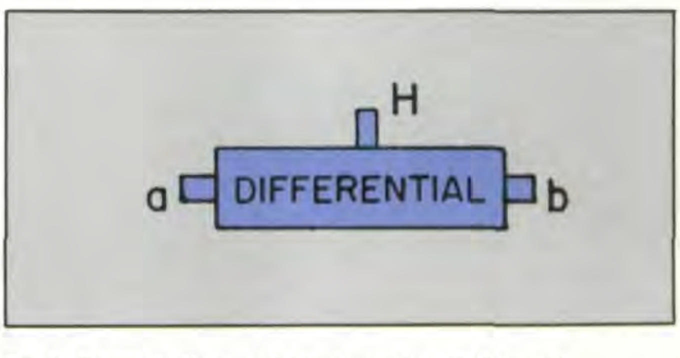

Fig. 2 – Schematic diagram of a fundamental gear differential

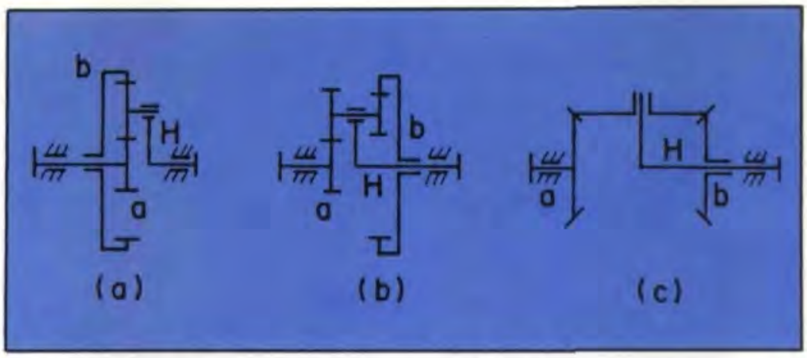

Fig. 3 – Three examples of the $2K - H(-)$ type of differential

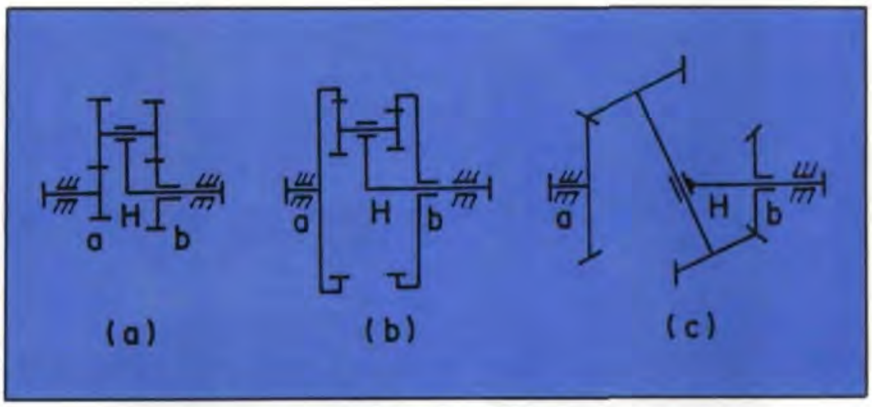

Fig. 4 – Three examples of the $2K - H(+)$ type of differential

1, then from a to b is a speed-up or "overdrive". We define a high-speed ratio as occurring when either the absolute value of a reduction speed ratio is very large or the absolute value of an overdrive speed ratio is very small. For example, both $|r_{ab}| = |N_a/N_b| = 1000$ and $|r_{ba}| = |N_b/N_a| = 1/1000$ are considered as high speed ratios, and the lowest possible speed ratio is therefore $|r| = 1$.

If the speed ratio is relative to a third member, the relative speed ratio should be used, and a superscript should be added to the symbol with two subscripts. For example, the relative speed ratio of a and b to H is defined as,

$$r^h_{ab} = \frac{N_a - N_h}{N_b - N_h} = 1/r^h_{ba} \tag{1a}$$

In the same way,

$$r^b_{ah} = 1/r^b_{ha} = \frac{N_a - N_b}{N_h - N_b} \tag{1b}$$

$$r^a_{bh} = 1/r^a_{hb} = \frac{N_b - N_a}{N_h - N_a} \tag{1c}$$

Thus we can get,

$$r^h_{ab} + r^b_{ah} = \frac{N_a - N_h}{N_b - N_h} + \frac{N_a - N_b}{N_h - N_b} = 1 \tag{2a}$$

$$r^h_{ba} + r^a_{bh} = 1 \tag{2b}$$

$$r^b_{ha} + r^a_{hb} = 1 \tag{2c}$$

Expressions (2) are the fundamental kinematic relations of a differential from which other more complex formulas can be derived.

Basic Speed Ratio. In many articles,[2, 5, 6, 10] the term "basic ratio of a differential" has been used, but for the purpose of this article, we will define the term more specifically than is usually done. The basic ratio of a differential should express the specific features of the differential gearing and be convenient for use.

There is only one speed ratio that can not only be related to the size, but also provide the basic characteristics of a differential gearing. It is to be named the *basic speed ratio* R_o,

$$R_o = r^h_{ah}$$

(Note, however, that the reciprocal r^h_{ba} could be used as alternative if so desired.)

The relative speed ratio of a and b *to* H is based on considering H as relatively fixed. It, therefore, can be determined in the same manner as that of a conventional gear train, and the relationships of teeth or diameters can be used.

The basic speed ratio can be calculated as

$$R_o = r^h_{ab} = (-1)^p \frac{Z_b \cdot Z_b' \ \ldots}{Z_a \cdot Z_a' \ \ldots} \tag{3}$$

where:

$Z_a, Z_a', \ldots$ = numbers of teeth of the driving gears from a to b,

$Z_b, Z_b', \ldots$ = numbers of teeth of the driven gears from a to b.

p = number of pairs of external gearing from a to b.

Basic Types of Epicyclic Gearing. A central gear K is defined as one whose axis continuously coincides with the common central axis of the differential.

There are two main types of epicyclic differential: $2K - H(-)$ as shown in Fig. 3, and $2K - H(+)$ as shown in Fig. 4. $2K$ means two central gears, and the single H means one carrier with planet gears. The '+' denotes $R_o > 0$, and '−'

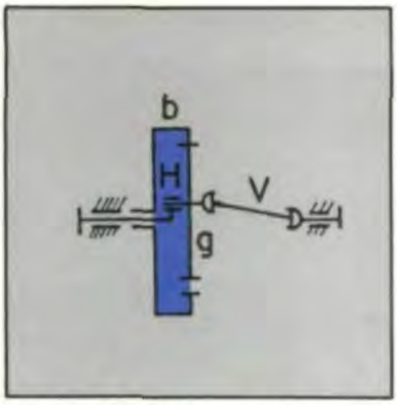

Fig. 5 – The KHV type of differential

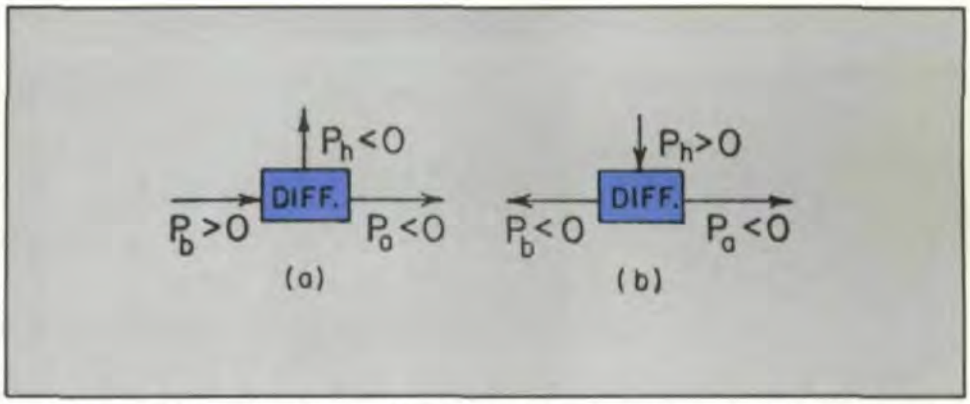

Fig. 6 – Changes in power flow directions that may occur when speed ratios are varied (with independent connections for the three differential elements)

means $R_o < 0$. As shown in Fig. 5, a relatively new type of differential is the KHV, consisting of only one central gear, one carrier, and an equal angular velocity mechanism V, where V has the same angular velocity as the planet gear g. It is compact in structure, light in weight, and with optimum design techniques, can often provide a higher efficiency.[12] It is, therefore, a very promising type of gearing for some applications. Since there is only one pair of internal gears, the basic ratio R_o is positive. Some characteristics of the KHV type are similar to those of a $2K - H(+)$ type. Since the three basic members of a KHV are b, H, and g (or V), all the previous and following equations are valid for it if g is substituted for a.

Efficiency. Power equals the product of torque and angular velocity, or the product of force and linear velocity.

We define input power P_{in} as positive, and both the output power P_{out} and the frictional power P_f as negative.

Conventionally, efficiency is a positive value, therefore, sometimes a minus sign or absolute value; symbol must be used in the efficiency formulas, such as:

$$\eta = \frac{-P_{out}}{P_{in}} = \frac{P_{in} - |P_f|}{P_{in}} = 1 - \frac{|P_f|}{P_{in}} \tag{4a}$$

and

$$\eta = \frac{P_{out}}{P_{out} + P_f} = \frac{1}{1 + P_f/P_{out}} \tag{4b}$$

Power Lost in Friction

If power's lost in friction, simply called frictional power, can be evaluated, it is easy to calculate the efficiency. The principle adopted here is the concept of relative motion, the same method as used for dealing with the kinematic relationships.

Frictional power is a function of torque and relative angular velocity. Let us observe two systems, a differential and a differential with its carrier H assumed relatively fixed. The angular velocities of the latter system are $N_a - N_h$, $N_b - N_h$, $N_g - N_h$, $N_h - N_h$, . . . But the relative angular velocity of any two members, for example of a and g $(N_a - N_h) - (N_g - N_h) = N_a - N_g$, is the same as that in the former system, so it is apparent that the two systems provide the same relative angular velocities between each pair of meshed gears. Because torque is independent of motion, the torque of each element is not affected by whether or not H is relatively fixed. Consequently, a useful conclusion can be drawn: the frictional power P_f of a differential can be calculated in all cases by assuming the carrier H to be relatively fixed.

It is convenient to use the concept of latent power. With H relatively fixed, we define

$$P_a^h = T_a (N_a - N_h) \tag{5}$$

and

$$P_b^h = T_b (N_b - N_h) \tag{6}$$

There exist two possibilities. The first is that a is the driving member (input) and b is the driven member (output) when H is relatively fixed, i.e., $P_a^h > 0$ and $P_b^h < 0$; where P_a^h and

P_b^h symbolize the powers of a and b when H is assumed to be relatively fixed. Strictly speaking, they are not real powers, but since they have the same dimensions as power it is convenient to refer to them as latent powers. Applying equation (4) to the case of H relatively fixed.

$$\eta_{ab}^h = 1 - \frac{|P_f|}{P_a^h} \tag{7}$$

or

$$\eta_{ab}^h = \frac{1}{1 + P_f / P_b^h} \tag{8}$$

The choice between equations (7) and (8) depends on whether P_a^h or P_b^h is available. Then,

$$|P_f| = (1 - \eta_{ab}^h) P_a^h = (1 - \eta_{ab}^h) T_a (N_a - N_h) \tag{9}$$

or

$$|P_f| = (1 - \eta_{ab}^h) P_b^h / \eta_{ab}^h = (1 - \eta_{ab}^h) T_b (N_b - N_h) / \eta_{ab}^h \tag{10}$$

where the superscript h means that H is relatively fixed, and the subscript ab denotes the power flow is from a to b.

The relationship between torques can be obtained as follows:

$$\eta_{ab}^h = \frac{-P_b^h}{P_a^h} = \frac{-T_b (N_b - N_h)}{T_a (N_a - N_h)} \tag{11}$$

so

$$\frac{T_b}{T_a} = \frac{-\eta_{ab}^h (N_a - N_h)}{N_b - N_h} \tag{12}$$

The second possibility is that b is input and a is output when H is assumed to be relatively fixed, i.e., $P_b^h > 0$ and $P_a^h < 0$. In this case,

$$\eta_{ba}^h = 1 - |P_f| / P_b^h \tag{13}$$

or

$$\eta_{ba}^h = \frac{1}{1 + P_f / P_a^h} \tag{14}$$

Then

$$|P_f| = (1 - \eta_{ba}^h) P_b^h = (1 - \eta_{ba}^h) T_b (N_b - N_h) \tag{15}$$

or

$$|P_f| = (1 - \eta_{ba}^h) P_a^h / \eta_{ba}^h = (1 - \eta_{ba}^h) T_a (N_a - N_h) / \eta_{ba}^h \tag{16}$$

For the torque relationship,

$$\eta_{ba}^h = \frac{-P_a^h}{P_b^h} = \frac{-T_a (N_a - N_h)}{T_b (N_b - N_h)} \tag{17}$$

or

$$\frac{T_a}{T_b} = -\eta_{ba}^h \frac{(N_b - N_h)}{(N_a - N_h)} \tag{18}$$

In the same way, expressions of η_{ah}^b, η_{ha}^b, η_{bh}^a, and η_{hb}^a could be derived, but only η_{ab}^h or η_{ba}^h can be determined in a direct manner. As shown in the foregoing, one of these two must be used to obtain a solution. This is the reason that we define either r_{ab}^h or r_{ba}^h as the basic speed ratio R_o.

When the carrier H is relatively fixed, certain features of a differential are similar to those of conventional gearing. Thus, formulas from[7, 8] or relevant handbook data available for conventional gearing can be used to calculate η_{ab}^h or η_{ba}^h.

The only remaining question is: when H is assumed relatively fixed, which one of the two efficiencies should be used, i.e., is a or b the input?

Let

$$S_a = P_a^h / P_a = T_a (N_a - N_h) / T_a N_a = 1 - N_h / N_a \tag{19}$$

$$S_b = P_b^h / P_b = T_b (N_b - N_h) / T_b N_b = 1 - N_h / N_b \tag{20}$$

where S is the ratio of the power assuming the carrier H relatively fixed to the actual power.

Usually the speed ratios N_h/N_a and N_h/N_b are known. If the sign of either P_a or P_b is known, then by means of equations (19) or (20) the sign of P_a^h or P_b^h can be determined. When $P_a^h > 0$ or $P_b^h < 0$, then η_{ab}^h and equations (7-12) should be used. When $P_b^h > 0$ or $P_a^h < 0$, η_{ba}^h and equations (13-18) should be used. Thus P_f will be obtained.

Efficiency of the Differential

After P_f is available and if P_{in} or P_{out} is known, then the

Nomenclature

- K = ratio of CVU output power to input power of total system
- K_o = ratio of CVU output power to input power of total system with friction assumed zero
- N = rotational speed
- P = power
- P_a^h = latent power of member a
- P_f = frictional power loss in differential
- P_{fv} = frictional power loss in CVU
- P_{in} = input power
- P_{out} = output power
- r = angular speed ratio
- r_{ab} = angular speed ratio, N_a/N_b
- r_{ab}^h = relative speed ratio $(N_a - N_h)/(N_b - N_h)$
- R = relative speed ratio of members 3 and 1 to member 2, $(N_3 - N_2)/(N_1 - N_2)$
- R_o = basic speed ratio of a differential, r_{ab}^h or r_{ba}^h
- S = ratio of power assuming H relatively fixed to actual power
- T = torque
- V = speed ratio of CVU
- Z = number of teeth on a gear
- η = efficiency
- η_{ab}^h = efficiency from a to b, assuming H relatively fixed
- η_d = efficiency of differential
- η_{oa} = overall efficiency
- η_v = efficiency of CVU

Subscripts and Superscripts

- a = member a of a differential
- b = member b of a differential
- g = planet gear g of a differential
- h = carrier H of a differential

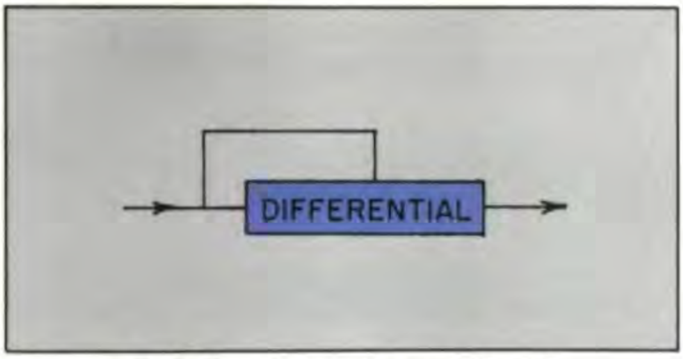

Fig. 7—Power input coupling to a differential

efficiency of the differential can be calculated by means of equation (4). However, we should first determine which of the three members (a, b, and H) is or are the input and output.

The torque equilibrium requirement is valid whether friction is omitted or is taken into account (since the basic differential has no torque reaction to ground) is:

$$T_a + T_b + T_h = 0 \qquad (21)$$

Using equation (21) in combination with equations (12) or (18) allows two equations related to torques to be obtained, so the relationship between any two torques can be determined.

Power is the product of torque and angular velocity,

$$P_a = T_a \cdot N_a, \quad P_b = T_b \cdot N_b, \quad P_h = T_h \cdot N_h \qquad (22)$$

Therefore, the relationship between each two powers can also be calculated.

If the sign of one of the three powers is given, for example, $P_a < 0$ (i.e., a is output), the direction of the other two can be obtained through equation (22). If, for example, $P_b < 0$ and $P_h > 0$ (i.e., b is another output and H is input) the differential efficiency is obtained from equation (4) as

$$\eta_d = \frac{P_h - |P_f|}{P_h}$$

or

$$\eta_d = \frac{|P_a| + |P_b|}{P_h}$$

However, it is not as simple as the case of planetary gearing, which has only one degree of freedom. For example, if b is fixed and a is output, then H must always be the input independent of speed ratio, and vice versa.

Differential gearing has two degrees of freedom. Two of the three members can be input and the other output, and vice versa, so there are six different possible combinations. Moreover, these relationships do not always remain the same throughout all the speed ratios needed. For example, if $r^h_{ab} = -1.7$ and $P_a < 0$ (a is output) are given, then when $N_a/N_b = -0.03$ we find $P_b/P_a = -59.6$ and $P_h/P_a = 57.5$, i.e., b is input and H is output (Fig. 6a). When $N_a/N_b = 0.05$; however, we find $P_b/P_a = 53.8$ and $P_h/P_a = -55.9$, i.e., b becomes output and H turns into input (Fig. 6b). Therefore, when powers are connected separately to the three members (Fig. 6), care must be taken to determine whether the power signs will change during the speed ratio range being used. If they do change, it is difficult to arrange the power connection of the differential. Consequently, it is impossible to get the general formulas available for all speed ratios. For example, in his article "Power Flow and Loss in Differential Mechanisms",[10] Macmillan has derived six general efficiency formulas. Although quite useful, they can only be valid for planetary gearing, not for a differential, since they require one of the three members of an epicyclic gearing to be absolutely fixed and not just relatively fixed. Consequently, the gearing operates with only one degree of freedom, and strictly speaking, two of the six formulas with fixed carrier are equivalent to those for conventional gearing.

Split-Path Transmissions Efficiency

To generate formulas that are valid for all speed ratios, it is necessary to couple two of the differential members together rather than to connect power to each element separately. It is most common to use the power input coupled type of system (Fig. 7). A useful transmission for automobiles and other mechanical applications is the input-coupled scheme shown in Fig. 8, where the CVU is a continuously variable speed ratio unit, such as a variable V-belt drive, a Perbury traction drive or some similar device.[1, 3, 6]

If we do not include the possibility of regenerative braking, member 3 in Fig. 8 is always the output ($P_3 = P_{out}$) and P_{in} is always the input. Depending on the system parameters and the speeds of the three differential elements, there are three possibilities: (a) $P_1 > 0$ and $P_2 > 0$, (Fig 8a) (b) $P_1 < 0$ and $P_2 > 0$, producing what is known as positive power recirculation through the CVU (Fig 8b), and (c) $P_1 > 0$ and $P_2 < 0$, producing negative power recirculation (Figure 8c).

In all three cases considered, the condition that power is

Fig. 8—An input-coupled split-path CVT showing the three power flow possibilities

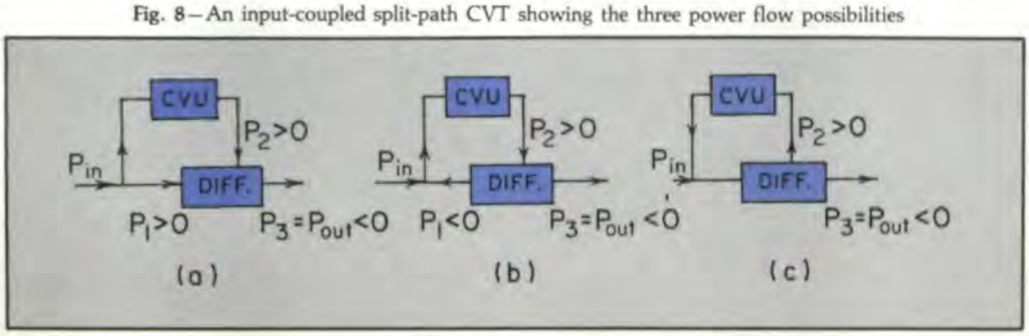

Table 1

Six Basic Types of Differential Connection and Nine Combinations

Six Types of Differential Connection	2 Members Which Interchange Positions								
	b, H			a, H			a, b		
1. 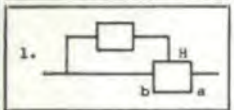	1			1			1		
2. 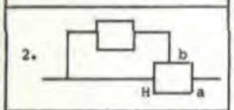	2				2			2	
3. 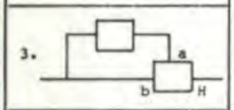		3		3					3
4. 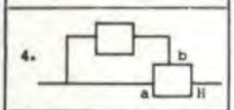			4		4				4
5. 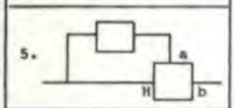		5				5		5	
6. 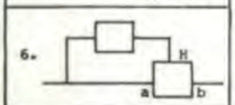			6			6	6		
Nine Combinations	I	II	III	IV	V	VI	VII	VIII	IX

input at "P_{in}" and output as "P_{out}" remains unchanged, so that the basic scheme of the transmission is the same. The overall speed ratio of the transmission is r, defined as $r = N_{out}/N_{in} = N_3/N_1$. The speed ratio of the CVU is $V = N_2/N_1$. Let R be the relative speed ratio of 3 and 1 and 2,

$$R = \frac{N_3 - N_2}{N_1 - N_2} = \frac{r - V}{1 - V}$$

then

$$V = (r - R)/(1 - R) \tag{23}$$

or

$$r = R + (1 - R)V \tag{24}$$

If the efficiency of the CVU is η_v and the power passing through the CVU at the differential side is $P_v = P_2$, then when $P_2 < 0$, the loss in the CVU is

$$|P_{fv}| = |P_v|(1 - \eta_v) \tag{25a}$$

and when $P_2 > 0$, it becomes

$$|P_{fv}| = |P_v|(1 - \eta_v)/\eta_v \tag{25b}$$

If the power loss through the differential is P_f, then the total loss is

$$P_{loss} = P_f + P_{fv} \tag{26a}$$

or

$$P_{loss}/P_{out} = P_f/P_{out} + P_{fv}/P_{out} \tag{26b}$$

The input power of the system is

$$P_{in} = -(P_{out} + P_{loss}) \tag{27a}$$

or

$$P_{in}/P_{out} = -(1 + P_{loss}/P_{out}) \tag{27b}$$

The overall efficiency of the system, which is more important than that of either the differential or the CVU alone will be

$$\eta_{oa} = -P_{out}/P_{in} \tag{28}$$

K is defined as the ratio of the input power of the CVU to the input power of the system. A positive P_v means that power passes from the CVU to the differential, and vice versa, so that

$$\text{when} \quad P_v < 0 \quad K = P_v/P_{in} \tag{29a}$$

$$\text{when} \quad P_v > 0 \quad K = P_v/\eta_v/P_{in} \tag{29b}$$

Example

To help clarify the foregoing, the following example is given: the differential is chosen to be a $2K - H(-)$ type as shown in Fig. 3a with $Z_b = 153$, $Z_a = 90$, so that $r^h_{ab} = -Z_b/Z_a = -153/90 = -1.7$,

1. The conditions given are: a is the ouput and H is the CVU; i.e., a at 3, H at 2, and b at 1, $R_o = r^h_{ab} = -1.7$, and $r = N_3/N_1 = N_a/N_b = -0.13$.
2. $V = N_2/N_1 = N_h/N_b$, and from equation (23), $V = (-0.13+1.7)/(1+1.7) = 0.581$, and $N_h/N_a = V/r = -4.47$.
3. $S_a = P^h_a/P_a = 1 - N_h/N_a = 5.47 > 0$. Since a is output, i.e., $P_a = P_{out} < 0$, then $P^h_a < 0$, i.e., a is driven when H is relatively fixed. Therefore, assuming $\eta^h_{ba} = 0.95$ and using equations (13)-(18), we get $T_b/T_a = 1.789$ and $T_h/T_a = -2.789$.
4. From equations (21) and (22), the power relationships are $P_b/P_a = -13.77$, $P_h/P_a = 12.48$, and $P_f/P_a = 0.288$. Since $P_a < 0$, then $P_b > 0$ and $P_h < 0$. Therefore, in the differential b is the input, a and H are outputs.
5. Now using equation (4a), we get the efficiency of the differential, $\eta_d = -(P_a+P_b)/P_b = 97.9$ percent.
6. If the efficiency of the CVU is assumed to be $\eta_v = 0.9$, then from equation (25) we get $|P_{fv}|P_{out}| = |P_h|(1 - \eta_v) / |P_{out}| = 12.48\,(1 - 0.9) = 1.248$, and from equation (26b) we obtain $P_{loss}/P_{out} = 0.288 + 1.248 = 1.536$.
7. The input power needed (equation (27b)) is $P_{in}/P_{out} = -(1+1.536) = -2.536$. The overall efficiency of the system can now be calculated as $\eta_{oa} = -P_{out}/P_{in} = -1/(-2.536) = 39.4$ percent.

Fig. 9—Power flow diagram of the example

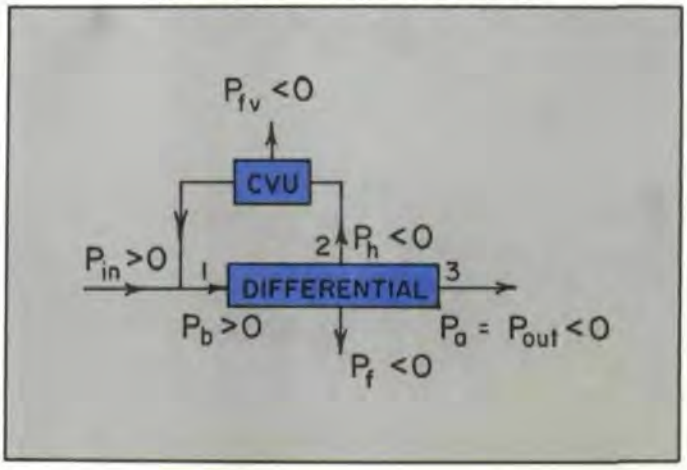

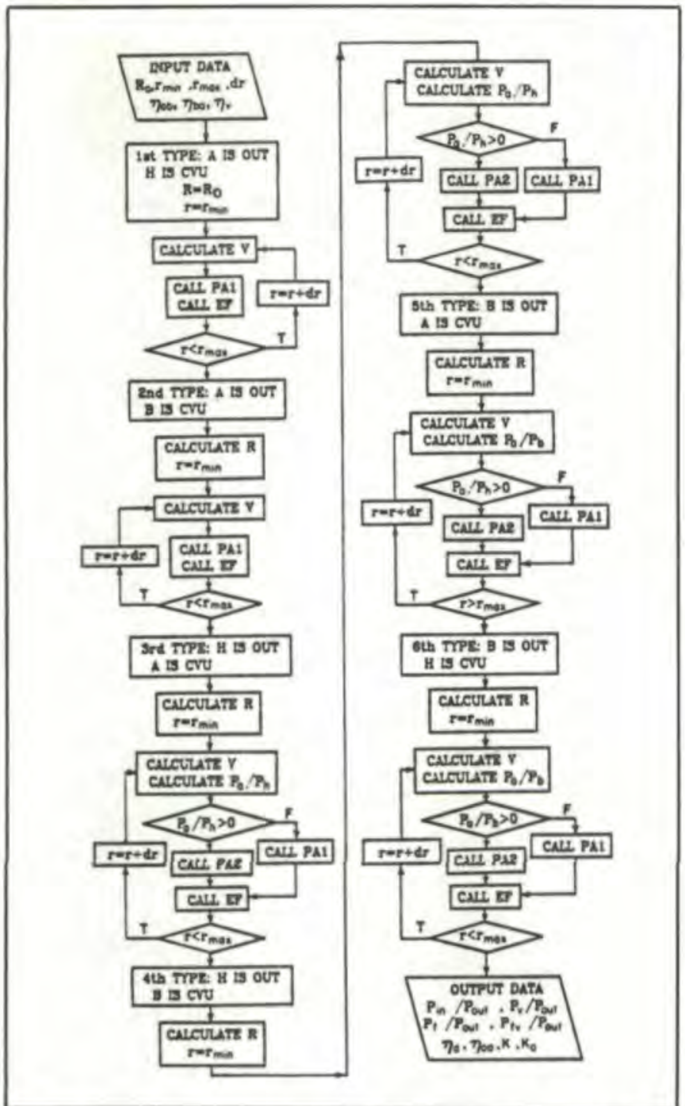

Fig. 10 – Computer flow chart calculating program for the input-coupled CVT

8. The portion of the input power passing through the CVU is $K = P_v/P_{in} = P_h/P_a/(P_{in}/P_{out}) = -4.92$. The minus sign means negative power recirculation.

9. The power flow directions are shown in Fig. 9.

Types of Connection

An important and interesting feature should be pointed out: there are six possible types of connection for the three basic members of each differential characterized by its basic speed ratio. Six different designs are available which enlarges the potential usage. For example, for a $2K-H(-)$ type with $R_o = r^h_{ab} = -1.7$, we have the following six possibilities as listed in Table 1:

1. If a is output and H is CVU (i.e., a at 3, H at 2, b at 1), then $R = r^h_{ab} = -1.7$ (as in the foregoing example).

2. If a is output and b is CVU (i.e., a at 3, H at 1, b at 2), then $R = r^b_{ah} = 1 - r^h_{ab} = 2.7$

3. If H is output and a is CVU, (i.e., H at 3, a at 2, b at 1), then $R = r^a_{hb} = 1/r^a_{bh} = 1/(1 - r^h_{ba})$, and $r^h_{ba} = 1/r^h_{ab}$, $R = 0.630$.

4. If H is output and b is CVU (i.e., H at 3, a at 1, b at 2), then $R = r^b_{ha} = 1/r^b_{ah} = 1/(1-r^h_{ab}) = 0.37$.

5. If b is output and a is CVU (i.e., b at 3, a at 2. H at 1), then $R = r^a_{bh} = 1 - r^h_{ba} = 1 - 1/r^h_{ab} = 1.59$.

6. If b is output and H is CVU (i.e., b at 3, a at 1, H at 2), then $R = r^h_{ba} = 1/r^h_{ab} = -0.59$.

Furthermore, if over the range of usage the type of connection can be changed, the design possibilities will be increased still further. Theoretically, 36 different designs are possible, provided that all three basic members can interchange positions. However, practical mechanisms for accomplishing this may be quite complicated. If only two of the three members are to interchange positions, there will be nine combinations as listed in Table 1, and the mechanisms for this will be much simpler[13]. For example, if b and H can interchange positions over the range of usage, there will be three combinations: *I*, *II*, and *III*. Referring to Table 1, combination *I* means that a is unchanged as the system output, but b and H interchange between the other two connections. The other eight combinations are similarly defined in Table 1. Note further that for any change in the basic speed ratio (i.e., changes in numbers of gear teeth), another six types and nine combinations can be obtained.

From the numerous possibilities, an optimum choice can be made to satisfy particular requirements. The details have been introduced in another article.[13]

Computer-Aided Design

To avoid arduous manual calculations, it is better to design

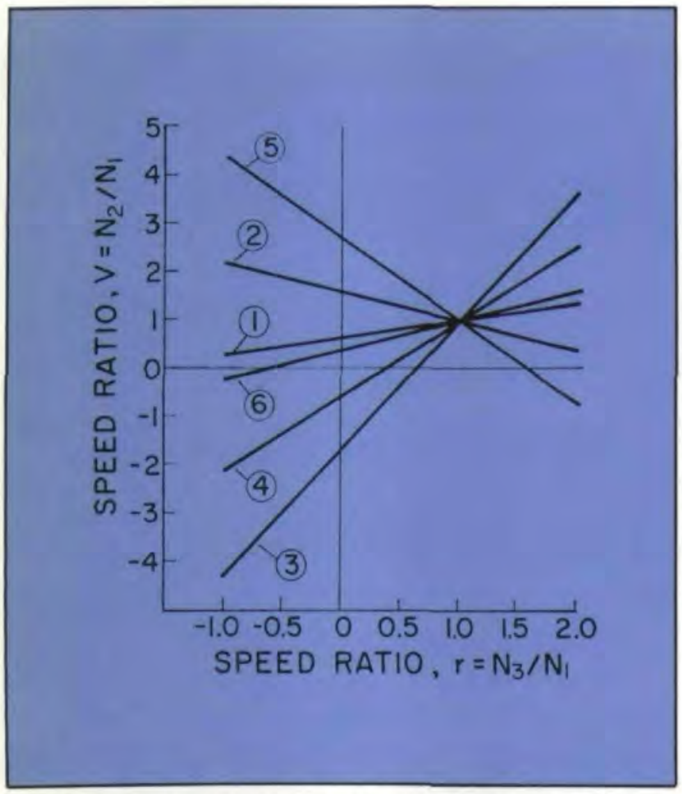

Fig. 11 – Required speed ratio relationships of the input-coupled CVT with $R_o = -1.7$, for the six ways of using the differential

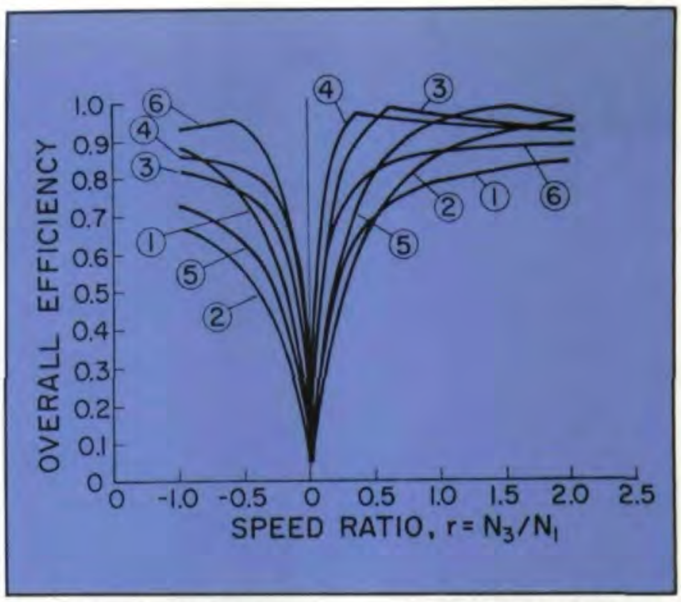

Fig. 12 – Efficiency characteristics of the input-coupled CVT for the six ways of using the differential ($R_o = 1.7$, $\eta_v = 0.90$, $\eta^h_{ab} = \eta^h_{ba} = 0.95$)

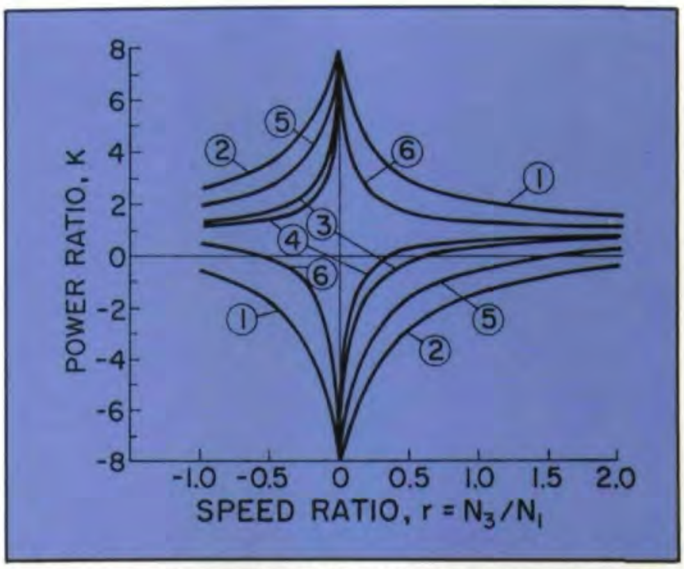

Fig. 13 – Fraction of power through the CVU (29) with friction losses taken into account

a general computer program to solve the problem. Two problems have been developed, the first one for calculation and the second for plotting curves. The flow chart of the calculating program is given in Fig. 10. Subroutines PA1 and PA2 are used to calculate torque and power relationships. Subroutine EF is designed to determine efficiency.

The input data are: (1) the basic speed ratio R_o, which represents the features of the differential gearing, (2) the range of speed ratios of the system, i.e., the maximum and minimum speed ratios, (3) the efficiency of the gearing with H assumed relatively fixed, and (4) the efficiency of the CVU. Each basic speed ratio (i.e., each specific differential) can provide six different split path CVT designs, and useful curves can be plotted for each.

For example, if the basic speed ratio $R_o = -1.70$ and it is a $2K-H(-)$ type, then the relationship between $V = N_2/N_1$ and $r = N3/N_1$ is as given in Fig. 11. If $\eta^h_{ab} = \eta^h_{ba}$ 0.95 and $\eta_v = 0.90$, the overall efficiency characteristics are as given in Fig. 12, and the fraction of power through the CVU as given by Fig. 13. The labeling from 1 to 6 of the different curves is the same as used earlier. With the friction loss assumed to be zero, as is normally the case in other CVT analysis articles, the fraction of power through the CVU is given the symbol K_o, and the curves of K_o are shown in Fig. 14. A comparison of Figs. 13 and 14 shows that K_o is quite different from K. Fig. 12 also shows that the overall efficiency is often far from 100 percent. It is concluded, therefore, that frictional losses must be included for realistic analysis. From the data and curves obtained, and the CVT characteristics needed, it may be possible to determine a better design. For example, if $N_3/N_1 = 0.5$ to 2.0 is used most of the time, curve 4 may be attractive, because it provides a higher efficiency and a smaller power through the CVU. However, if the available range of $V = N_2/N_1$ is smaller, it may be better to choose curve 6, because V varies only from 0.69 to 1.66, although the efficiency in this case would be lower.

Summary

Because of its compact structure, small size, capability of high speed ratios, and the differential action itself, differential gearing has been often employed in modern machinery. However, in many design analyses, an important index, mechanical efficiency, has been ignored. The assumption of

(continued on page 48)

Just "average" doesn't cut it anymore.

U.S. gear makers need a competitive edge. In these competitive times it takes above average performance, *and above average suppliers,* to survive.

ILLINOIS TOOLS helps provide that competitive edge:

☐ We're organized to get you the gear generating tools you need — *when you need them*.

☐ Our prices are surprisingly competitive and we are offering an expanded line of off-the-shelf standard gear tools.

☐ Fast response to your engineered special and prototype needs.

☐ Our products, which have continued to set the quality standard for the industry for more than 70 years, are your assurance of reliable, durable, high performance hobs, shaper cutters, master gears and worm gear hobs.

ILLINOIS TOOLS has established a Gear Tool Hotline to answer any questions and provide the latest information on gear tooling. Just call, TOLL FREE, 1-800-628-2220 (in Illinois, call 1-800-628-2221).

Our widely acclaimed Gear School also continues to keep America's gear technologists up to date on the state-of-the-art in gear making and gear inspection.

In gear making, competitive performance starts with the first cut. ILLINOIS TOOLS will help cut it with faster deliveries and lower costs!

If you're looking for a competitive edge, call us.

THE COMPETITIVE EDGE

ITW Illinois Tools

Gear Tool Specialists

An Illinois Tool Works Company
3601 W. Touhy Ave./Lincolnwood, IL 60645/312-761-2100

GEAR TOOL HOTLINE: Phone TOLL FREE 1-800-628-2220. In Illinois call: 1-800-628-2221.

Visit us at IMTS Booth #2219

CIRCLE A-19 ON READER REPLY CARD

Effect of MoS_2 Films on Scoring Resistance of Gears

Y. Terauchi
Hiroshima University—Hiroshima, Japan
H. Nadano
M. Kohno
Kure Technical College—Hiroshima, Japan

Introduction

Gears are currently run at high speed and under high load. It is a significant problem to develop lubricants and gears with high load-carrying capacity against scoring. The particles of molybdenum disulfide have been considered to increase the scoring resistance of the gears. The wear characteristics and the scoring resistance of the gears lubricated with MoS_2 paste and MoS_2 powder have been investigated.[1] However, there are few investigations on the performance of the gears coated with MoS_2 film with respect to scoring.

In this report, scoring tests of the gears coated with the MoS_2 film that is about 10 μm thick are carried out with a power-circulating gear machine, and the effect of the MoS_2 film on the scoring resistance and the wear characteristics of the gears are examined. Further, the surface temperature of the gears coated with the MoS_2 film is evaluated by the flash temperature equation of case-hardened gears and the effect of the MoS_2 film on the scoring resistance of the gears is examined from a standpoint of the surface temperature.[2]

Equation of Flash Temperature Rise of Gear Tooth

The equation for calculating the flash temperature rise at the meshing faces of case-hardened gears in which the thermal properties in the surface-hardened layer are different from those in the core of the gear tooth can be rewritten by using the dimensionless parameters as follows:

$$\begin{aligned}\theta_f = \frac{2\kappa_1 q_0}{\pi K_1 V}\Bigg[\Bigg[&4\sqrt{2\pi\beta L}\Bigg[\beta\left(\frac{1}{3}-\frac{2}{15}\beta\right)\\
&\times\left\{1+2\sum_{n=1}^{\infty}\alpha^n \exp\left(-\frac{2n^2\delta^2 L}{\beta}\right)\right\}\\
&+\left(\frac{4}{3}-\frac{6}{5}\beta\right)\delta^2 L\sum_{n=1}^{\infty}\alpha^n n^2 \exp\left(-\frac{2n^2\delta^2 L}{\beta}\right)\\
&-\frac{8}{15}\delta^4 L^2\sum_{n=1}^{\infty}\alpha^n n^4 \exp\left(-\frac{2n^2\delta^2 L}{\beta}\right)\Bigg]\\
&-4\pi\delta L\sum_{n=1}^{\infty}\alpha^n n\left\{2\beta-\beta^2+\frac{8}{3}n^2\delta^2 L(1-\beta)-\frac{16}{15}n^4\delta^4L^2\right\}\\
&\times \operatorname{erfc}\left(\frac{\sqrt{2L}n\delta}{\sqrt{\beta}}\right)\Bigg]\Bigg] \qquad (1)\end{aligned}$$

where $\alpha=(1-\omega)/(1+\omega)$, $\operatorname{erfc}(\gamma)=1-\operatorname{erf}(\gamma)$,

$$\operatorname{erf}(\lambda)=\frac{2}{\sqrt{\pi}}\int_0^{\lambda}\exp(-\xi^2)d\xi.$$

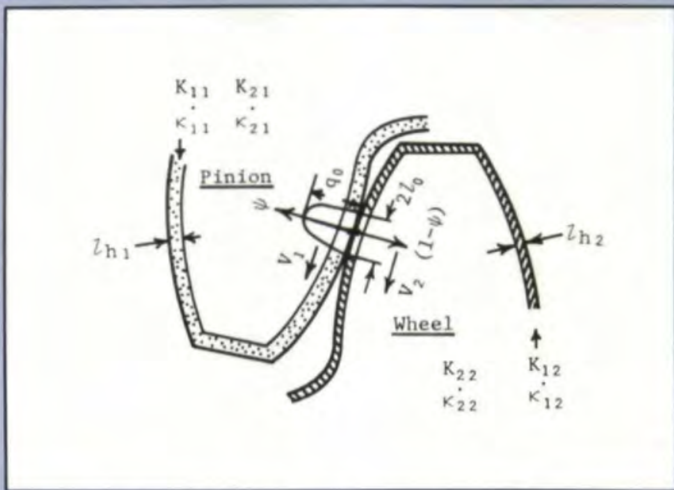

Fig. 1—Schema of mating condition of gear teeth

Fig. 1 shows a schema of the mating condition of the gear teeth. In this figure, the subscripts 1 and 2 relate to the pi-

---

AUTHORS:

MR. YOSHIO TERAUCHI *is a Professor at the University of Kyoto. He has performed research work in the field of deformation and strength of mating teeth of gears. Terauchi has published numerous papers on rolling contact problems, gear lubrication, scoring, and gear noise. Current research interests include vibration and scoring resistance of bevel gears and performance of the traction drive.*

HIROMASA NADANO *is a Professor at Kure Technical College. Present interests and areas of study include the effect of heat in oil films on tribological phenomena. Academically, he earned a Doctorate in Engineering from the University of Kyoto.*

MR. MASAKI KOHNO *is a lecturer at Kure Technical College. Kohno was awarded a Doctorate in Engineering from Hiroshima University. His major research efforts include scoring and surface roughness.*

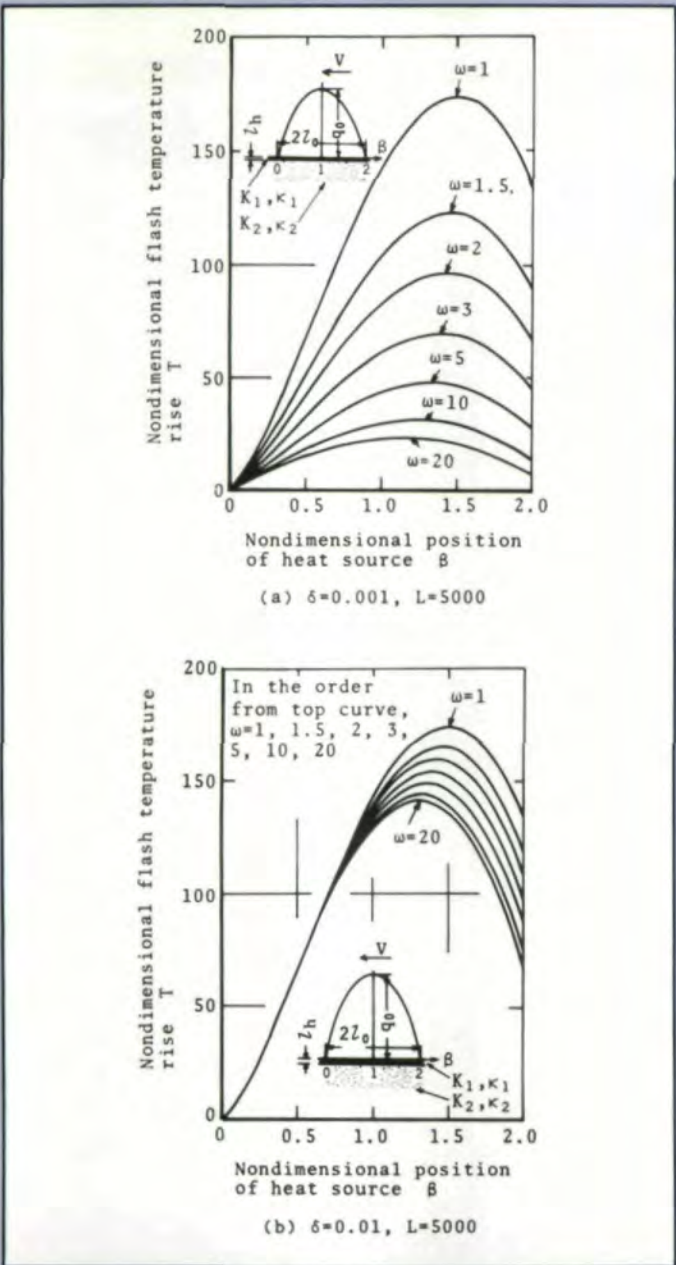

Fig. 2—Relation between nondimensional flash temperature rise and nondimensional position of heat source

nion and the wheel, respectively. The distribution of heat intensity is assumed to be parabolic. Therefore, the value of q_0 is given by,

$$\mu\delta_0 P_n |V_1 - V_2| = 4q_0 l_0/3 \tag{2}$$

The equations of the surface temperature at the meshing faces of the pinion and the wheel are derived from equation (1) as follows:

$$\left.\begin{aligned} \theta_{f_1} &= \frac{2\kappa_{11}q_0}{\pi K_{11}V_1}T_1 \\ \theta_{f_2} &= \frac{2\kappa_{12}q_0}{\pi K_{12}V_2}T_2 \end{aligned}\right\} \tag{3}$$

When the rates of the heat quantity flowing from the conjunctional area into the mating teeth of the pinion and the wheel are expressed by ψ and $1-\psi$, the surface temperature at the meshing faces of the pinion is equivalent to that of the wheel. Therefore, the value of ψ is given by

$$\psi = \frac{\kappa_{12}K_{11}T_2}{\kappa_{11}K_{12}T_1V_2/V_1 + \kappa_{12}K_{11}T_2} \tag{4}$$

The surface temperature at the meshing faces is given by

$$\theta_f = \frac{\kappa_{12}T_1T_2}{\kappa_{11}K_{12}T_1V_2/V_1 + \kappa_{12}K_{11}T_2}\,\frac{2\kappa_{11}q_0}{\pi V_1} \tag{5}$$

Calculated Results

For example, Figs. 2(*a*) and (*b*) show the relation between the flash temperature rise and the position of the heat source, expressed in terms of the dimensionless parameters T and β, respectively. In this figure, $\omega=1$ indicates that the thermal properties in the surface layer are equivalent to those in the core, and the maximum value of T occurs at $\beta=1.5$. In contrast, $\omega>1$ indicates that the thermal properties in the surface layer are worse than those in the core. The maximum value of T occurs at $1<\beta<1.5$, and the position where the *maximum value of T appears moves toward the vicinity of* the center of the heat source with an increasing value of ω.

Figs. 3(*a*) and (*b*) show the relation between the maximum

(continued on page 22)

Nomenclature

a = acceleration due to oscillation of gear box, m/s^2
g = gravitational acceleration = 9.8 m/s^2
K_1 = thermal conductivity in the surface layer of gear tooth, W/(m K)
K_2 = thermal conductivity in the core of gear tooth, W/(m K)
L = nondimensional velocity of heat source = $Vl_0/(2\kappa_1)$
l_h = thickness of surface layer, m
l_0 = a half of the band length of Hertzian contact zone, m
n_1 = rotational speed of pinion, rpm
P = normal load per unit ball, N
P_n = normal load per unit face width, N/m
q_0 = maximum value of heat intensity generated per unit time, W/m^2
T = nondimensional flash temperature rise = $\pi K_1 V\theta_f/(2\kappa_1 q_0)$
V = sliding velocity, m/s
β = nondimensional position of heat source = rV/l_0
δ = nondimensional thickness of surface layer = l_h/l_0
δ_0 = load-sharing
θ_f = flash temperature rise, K
θ_0 = bulk-temperature, K
k_1 = thermal diffusivity in the surface layer of gear tooth, m^2/s
k_2 = thermal diffusivity in the core of gear tooth, m^2/s
μ = coefficient of friction
r = time, s
ω = ratio of thermal contact coefficient of surface layer and core = $(K_2/\sqrt{k_2})/(K_1/\sqrt{k_1})$


THE NEW GLEASON
G-MAXX™
BEVEL GEAR GENERATOR
GLEASON
Visit us at IMTS Booth #6333 McCormick North

THE FIRST TRULY UNIVERSAL BEVEL GEAR GENERATOR EVER MADE

First ever CNC bevel gear generator.

First with two *and* three axis geometries.

First with such superior machine accuracy.

The new Gleason G-MAXX™ 2010 bevel gear generator can give you strong, quiet, high quality gears more productively, more cost efficiently than any other generator ever made.

First In Flexibility

You get three axis geometry for quick, accurate, continuous hobbing. You get a completed gear and pinion in one chucking.

You also get two axis geometry for cutting, grinding and hard finishing by the intermittent face mill process.

The new Gleason G-MAXX generator is designed to either stand alone or function in an automated systems manufacturing environment.

No other generator ever made gives you such choices.

First In Electronics

You program and store your machine settings with Computerized Numeric Control. CNC controls the speed and position for cutter, cradle, workspindle, and sliding base to drastically reduce your set-up time. You can handle smaller, more diverse runs more productively.

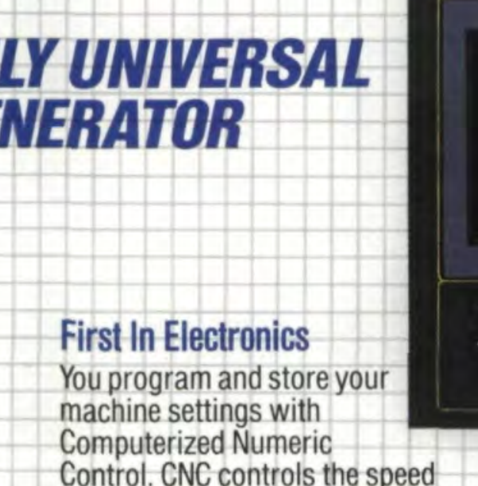

Drive is controlled electronically, not mechanically. Just 14 gears precisely transmit all motion. A shorter drive train maximizes the accuracy and finish of your gear.

First In Tooling

For continuous hobbing, alternate blade design of our exclusive TRI-AC™ cutter allows for more blade groups per head. You can cut far faster than with conventional cutters. Coated front blade surface reduces tool wear so you can cut far more pieces before sharpening. When you do sharpen, coating stays intact. You get a higher quality finish that requires up to 50% less lapping time.

First In Savings

It all adds up. Prime flexibility, CNC control, high accuracy, fast setup, and high quality gear sets can elevate your productivity to greatly diminish your overall cost per piece. And that's the number one benefit to your bottom line.

Ask For A First Cut

We'll be happy to run a comparative manufacturing cost analysis based on your bevel gear needs. Talk to your Gleason representative or call us direct. 716-473-1000. Or write Gleason Works, 1000 University Avenue, Rochester NY 14692 USA. See for yourself all the cost efficient solutions the new Gleason G-MAXX 2010 Generator can bring to you.

GLEASON

G-MAXX and TRI-AC are Trademarks of Gleason Works

CIRCLE A-7 ON READER REPLY CARD

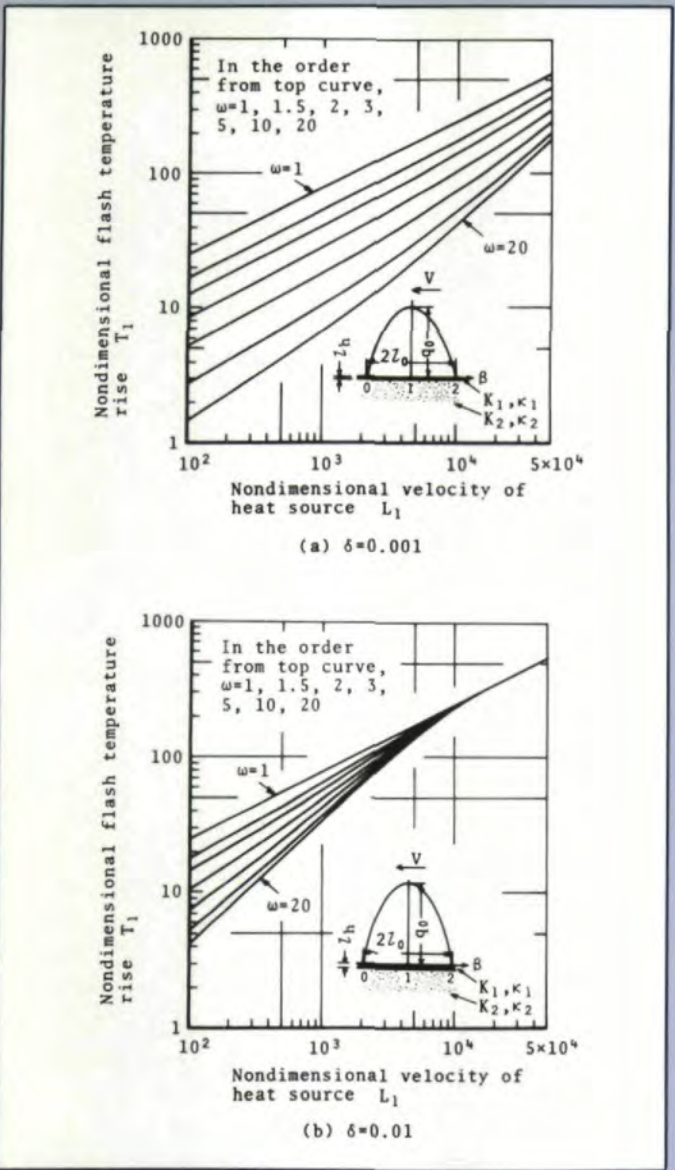

Fig. 3 – Relation between maximum value of nondimensional flash temperature rise and nondimensional velocity of heat source

value of the flash temperature rise and the velocity, expressed in terms of the dimensionless parameters T and L. When the thickness of the surface layer is smaller than the band length of the Hertzian contact zone as shown in Fig. 3(*a*), the effect of ω on the flash temperature rise is significant. In this article, the tooth surface of the gears was coated with the MoS_2 film whose thickness was a little larger than the surface roughness R_{max} of the tooth surface, and the difference between the thermal properties in the surface layer and those in the core is an important problem. The effect of ω on the flash temperature rise decreases with an increasing thickness of the surface layer.

Four Ball Tests

For investigating the seizure load and the frictional characteristics of the balls coated with MoS_2 film, tests have been carried out with a four-ball machine.

Test Balls. The diameter and the average sphericalness of the balls before coating with the MoS_2 film are 19.05 mm and 0.18 μm, respectively. The chemical compositions of ball material are given in Table 1. The balls were normalized at 443 K after quenched from 1173 K. The surface of the balls before coating had a Vickers microhardness of approximately 800 HV. The balls were coated with the MoS_2 film that was about 10μm thick, and the surface roughness of the balls was approximately 9 μm R_{max}.

Table 1 Chemical compositions of ball material

Composition %					
C	Si	P	S	Cr	Mn
0.98	0.32	0.019	0.007	1.40	0.42

Table 2 Combination of ball pairs

		Pair A	Pair B	Pair C	Pair D
MoS_2 coated	Upper ball (Rotating ball)	No	Yes	Yes	No
	Lower balls (Three fixed balls)	No	Yes	No	Yes

Lubricant. The balls were lubricated with number 140 turbine oil (a straight mineral oil without additives) with viscosities of 28×10^{-6} m²/s at 323 K and 8×10^{-6} m²/s at 363 K, and the oil temperature was controlled to 293 $\pm$ 2 K by the thermostat during all tests. The upper ball was immersed about 1/3 diameter deep into the oil bath.

Experimental Method. The four ball tests were carried out with stepwise increasing loads (the load P was increased by about 40 N increments at 30 s intervals) at a constant sliding velocity 0.29 m/s until the seizure of the balls occurred.

The combination of the balls consists of the four types of the ball pairs as shown in Table 2.

Test Results and Observations

Coefficient of Friction. Fig. 4 shows the relation between the coefficient of friction and the load at the sliding velocity 0.29 m/s. In this figure, the symbol S indicates the incipience of seizure.

Under comparatively low load (P<0.4 kN or the maximum Hertzian stress p_0<3.52 GPa), the coefficient of friction between ball pair A was the largest of all ball pairs, and the coefficient of friction between the balls coated with the MoS_2 film was considerably small. Therefore, the MoS_2 film is considered to play a significant role in decreasing the coefficient of friction. At the incipient stage of seizure, however, the coefficient of friction between the balls coated with the MoS_2 film was approximately equal to that between the balls without it since the MoS_2 film coated on the balls was completely torn out due to wear.

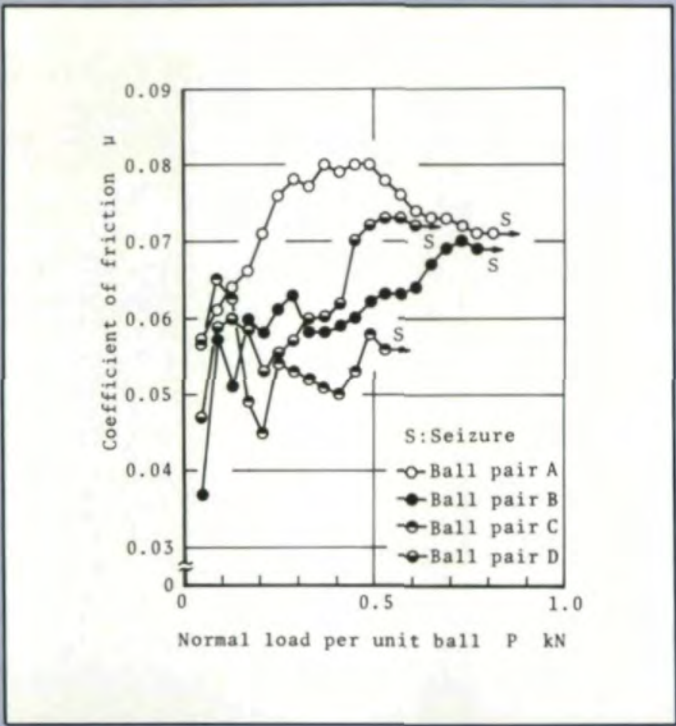

Fig. 4 – Relation between coefficient of friction and load

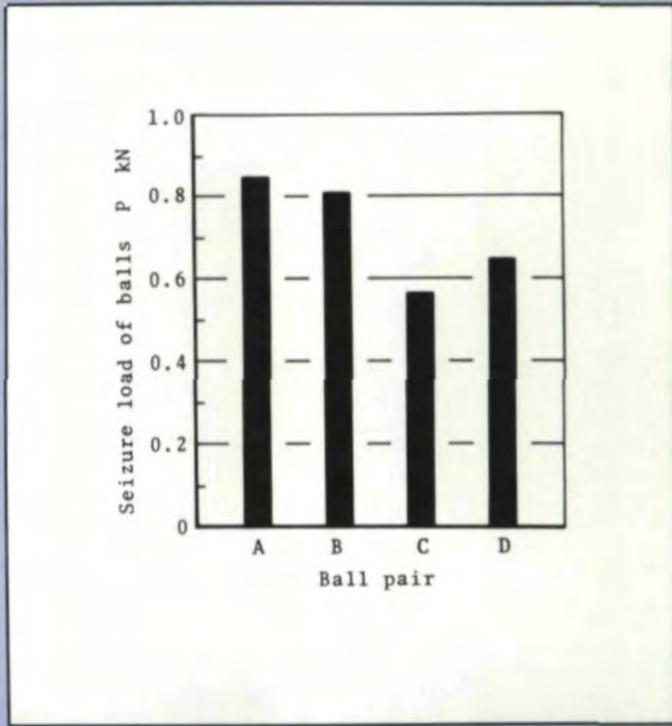

Fig. 5 – Seizure load of balls obtained with four-ball machine

(continued on page 26)

Table 3 Chemical compositions of tooth material

Composition %								
C	Si	Mn	P	S	Ni	Cr	Mo	Cu
0.18	0.28	0.80	0.014	0.019	0.08	0.99	0.16	0.09

Table 5 Combination of gear pairs

		Pair A	Pair B	Pair C	Pair D
MoS_2 coated	Pinion	No	Yes	Yes	No
	Wheel	No	Yes	No	Yes

Table 4 Data for test gears

	Pinion	Wheel
Number of teeth z	18	40
Center distance mm	116	
Pressure angle α_0	20°	
Module m mm	4	
Backlash Sn mm	0.5	
Face width B mm	10	
Effective face width Bf mm	7	
Tooth profile	Standard	
Pitch circle diameter d_0 mm	72	160
Outside diameter d_1 mm	80	168
Contact length mm	19.15	
Contact ratio ε	1.62	
Material	SCM 415H	

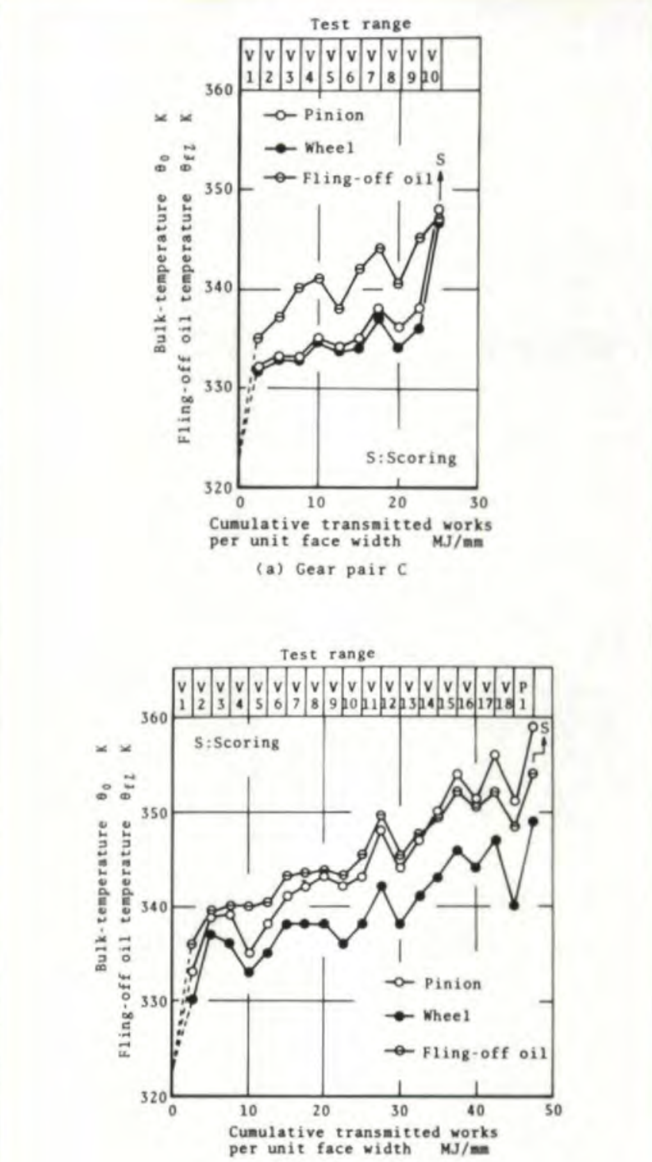

Fig. 6—Variations in bulk-temperature of gear teeth and fling-off oil temperature

Seizure Load. Fig. 5 shows the variation in the seizure load of the balls coated with the MoS_2 film or without it. The seizure load of the balls with ball pair B was not so much different from that with ball pair A, and little effect of the MoS_2 film could be recognized on the seizure load of the balls. Further, with ball pairs C and D, the seizure load of the balls was smaller than that with ball pair A, and it rather decreased due to the coating of the MoS_2 film.

Gear Tests

Scoring tests of the gears coated with MoS_2 film were run with a power-circulating gear machine. The effect of the MoS_2 film on the scoring resistance of the gears was investigated.

Test Gears. The test gears were made of chrome-molybdenum steel and case-hardened by gas-carburizing. The chemical compositions of tooth material are shown in Table 3. The working surface of the gears had a Vickers microhardness of approximately 720 HV. The gears were ground by a gear grinding machine as shown in Table 4. The single-pitch error and the tooth profile error of the gears were approximately 2 μm before coating with the MoS_2 film. The accuracy of the tooth profile of the gears before coating was of zero class, according to the Japanese Industrial Standard JIS B 1702. The surface roughnesses along the tooth trace of the pinion and the wheel before coating were about 2 μm R_{max}.

The combination of the gears consists of the four types of the gear pairs as shown in Table 5. The gear teeth were coated

Experimental Method. The scoring tests were carried out with the MoS_2 film that was about 10 μm thick after grinding, and the surface roughness after coating was approximately 9 μm R_{max}.

Lubricant. The test gears were lubricated with the same oil used for the four ball tests. The oil was sprayed onto the meshing faces at a rate of 0.6 L/min. The oil temperature was controlled to 323±2 K by the thermostat during all tests.

Table 6 (a) Speed data

Speed range	V-1	V-2	V-3	V-4	V-5	V-6	V-7	V-8	V-9	V-10	V-11	V-12	V-13	V-14	V-15	V-16	V-17	V-18
Rotational speed of pinion n_1 rpm	2000	2310	2644	3001	3381	3783	4208	4655	5125	5618	6133	6671	7231	7814	8420	9048	9699	10372
Peripheral velocity m/s	7.5	8.7	10.0	11.3	12.7	14.3	15.9	17.6	19.3	21.2	23.1	25.2	27.3	29.5	31.7	34.1	36.6	39.1
Cumulative transmitted works * MJ/mm	2.5	5.0	7.5	10.0	12.5	15.0	17.4	19.9	22.4	24.9	27.4	29.9	32.4	34.9	37.4	39.9	42.4	44.9

* The cumulative transmitted works are defined as the sum of the transmitted works per unit face width at the respective test ranges.

Table 6 (b) Load data

Load range	P-1	P-2	P-3	P-4	P-5	P-6	P-7	P-8	P-9	P-10
Tooth load Pn N/mm	278	290	302	314	327	339	352	364	377	390
Cumulative transmitted works MJ/mm	47.5	50.2	53.0	55.9	59.0	62.2	65.4	68.8	72.4	76.0

at stepwise increasing pinion speeds from V-1 to V-18 as shown in Table 6(*a*). The increment of the calculated value of the flash temperature rise was the same for the respective speed ranges under a constant load of P_n = 266 N/mm. When surface failure by scoring was not observed up to the speed range V-18, the tests were continued with stepwise increasing loads at a constant pinion speed of n_1=10372 rpm as shown in Table 6(*b*). The increment of the flash temperature rise per unit load range corresponds to that of the flash temperature rise per unit speed range.

The tests were run until the total number of pinion revolutions reached 4.4×10^4 at the respective ranges.

Scoring was detected by the following methods: (*a*) visual inspection of the tooth faces; (*b*) measurement of the surface roughnesses along the tooth trace and the tooth profile of the gears; (*c*) measurements of the bulk-temperature of the mating teeth and the fling-off oil temperature; (*d*) measurement of the acceleration due to oscillation of the gear box.

To measure the surface roughness along the tooth profile, the feeler set on the tooth profile testing machine was replaced with a thin cantilever in which a diamond needle was attached to the end of a plate spring that was 0.2 mm thick. The surface roughness was detected with a semiconductor strain gage that was attached to the root of the cantilever.

The bulk-temperature of the mating teeth was measured by pressing a contact-type thermister thermometer against the side of the tooth just after the test machine was stopped. Therefore, the bulk-temperature measured was considered to be a little lower than that in running.

The fling-off oil temperature was measured by thermocouples set up at a position opposite the mating position of the pinion. The distance between the hot junction of the thermocouples and the tip of the pinion was approximately 1 mm.

The acceleration due to oscillation of the gear box was measured by a piezoelectric accelerometer attached to the side of the test gear box.

The measurement of the acceleration due to oscillation was started 1 minute before each end of the respective test ranges, and the acceleration was recorded on the magnetic tape of a data recorder (characteristics of FM : 0 ~ 10 kHz) for about 30 s.

Test Results and Observations

Bulk-Temperature of Gear Tooth and Fling-Off Oil Temperature. For example, Fig. 6 shows the variations in the bulk-temperature of the gear teeth and the fling-off oil temperature with gear pair C (a pinion with the MoS_2 film and a wheel without it) and gear pair D (a pinion without the MoS_2 film and a wheel with it) until surface failure is caused by scoring. In this figure, the symbol S indicates the incipience of surface failure by scoring.

The values of the thermal properties of tooth material and MoS_2 material are shown in Table 7. As evident from equation (4), when the MoS_2 film-coated gear teeth with low thermal properties mate with the gear teeth without it, the rate of the frictional heat flowing into the meshing faces of the gears with the MoS_2 film is less than the gears without it. Thus, the bulk-temperature of the mating teeth coated with the MoS_2 film becomes lower than that of the gears without it.

With gear pair C, the difference between the bulk-temperatures of the mating teeth of the pinion and the wheel was insignificant, and the effect of the MoS_2 film could be recognized on the bulk-temperature of the mating teeth. The bulk-temperature suddenly increased by about 10 K at the incipience of surface failure by scoring. On the other hand, the fling-off oil temperature was higher than the bulk-temperature of the gear teeth.

With gear pair D, in contrast, the difference between the

Table 7 Values of thermal properties of tooth material[2] and MoS_2 material[3]

Material	Thermal conductivity K W/(m K)	Thermal diffusivity κ m^2/s
SCM 415H (373 K)	24	6.67×10^{-6}
MoS_2 (373 K)	0.14	6.88×10^{-8}

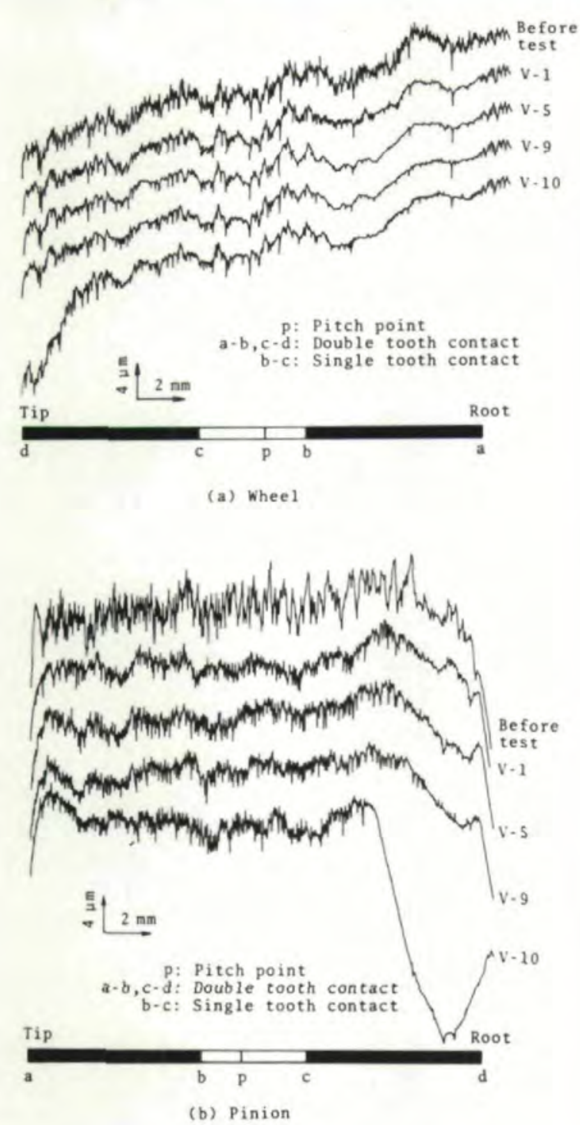

Fig. 7 – Variation in surface roughness along tooth profile with gear pair C

center of the face width with gear pair C is shown in Fig. 7. The variation in the surface roughness of the wheel before surface failure is caused by scoring was considerably small. On the other hand, the depth of a hollow occurring in the vicinity of the root of the pinion considerably increased with an increasing test range. The surface roughness along the tooth profile of the pinion coated with the MoS_2 film before tests was 8 μm R_{max}, and the surface roughness at the speed range V-1 was 3 μm R_{max} since the MoS_2 film coated on the tooth surface was torn out due to wear. However, the variation in the surface roughness after V-5 was considerably small.

A destructive surface failure by scoring occurred in the vicinity of the meshing position when the tip of the wheel mated with the root of the pinion. The EHD film thickness, calculated by Dowson's formula, at the meshing position at which destructive surface failure by scoring was observed, is 0.33 μm at V-10. Since the value of λ[4], defined as the ratio of the film thickness to combined surface texture, is approximately 0.9, the tests were run under mixed lubricating conditions.

For example, Fig. 8 shows the variation in the surface roughness of the tooth surface along the tooth trace in the vicinity of the tip of the wheel with gear pair D. The thickness of the MoS_2 film coated on the tooth surface of the wheel decreased by approximately 8 μm at V-1. After the test range exceeded V-11, the variation in the thickness of the MoS_2 film was considerably small. Surface failure by scoring occurred at the load range P-1, and a part of the base metal

Fig. 8 – Variation in surface roughness along tooth trace in the vicinity of tip of wheel gear pair D

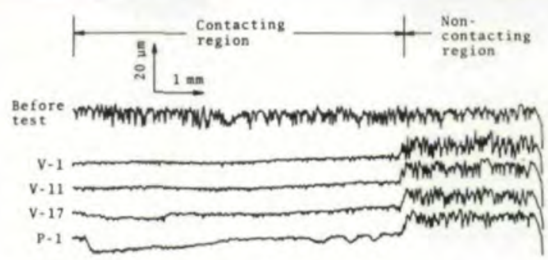

Fig. 8 Variation in surface roughness along tooth trace in the vicinity of the tip of wheel with gear pair D

Fig. 9 – Electron micrographs obtained with scanning X-ray microanalyzer at tip of wheel with gear pair D

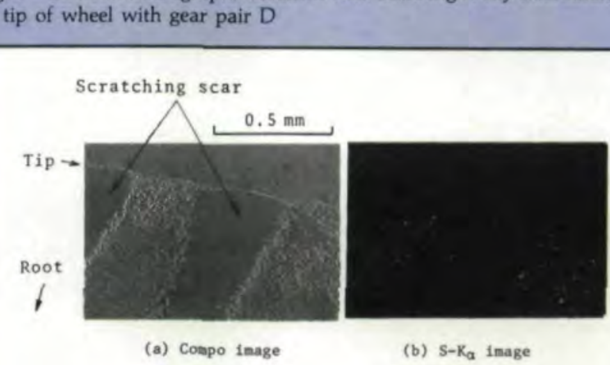

(a) Compo image (b) S-K_α image

bulk-temperatures of the mating teeth of the pinion and the wheel significantly increased with an increasing test range, and the bulk-temperatures of the pinion was approximately 10 K higher than that of the wheel at the incipience of surface failure by scoring. On the other hand, the fling-off oil temperature was not so much different from the bulk-temperature of the pinion.

Surface Roughness. The variation in the surface roughness of the tooth surface along the tooth profile at the

(continued on page 30)

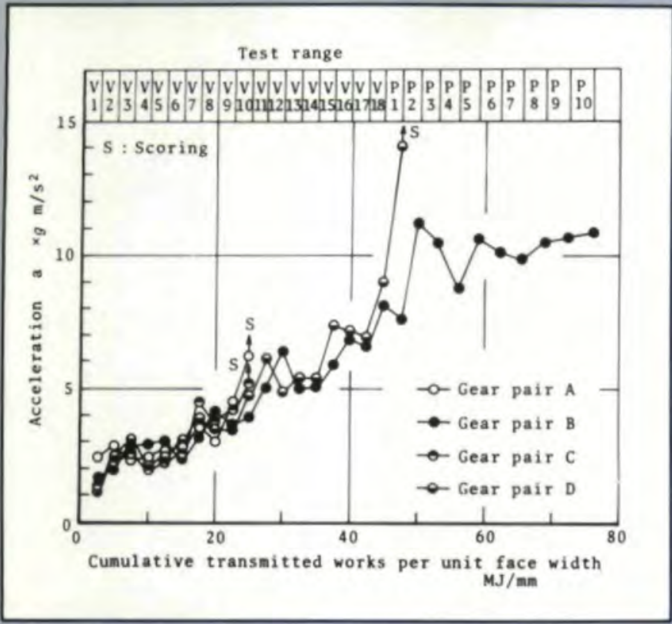

Fig. 10 – Variation in acceleration due to oscillation of gear box

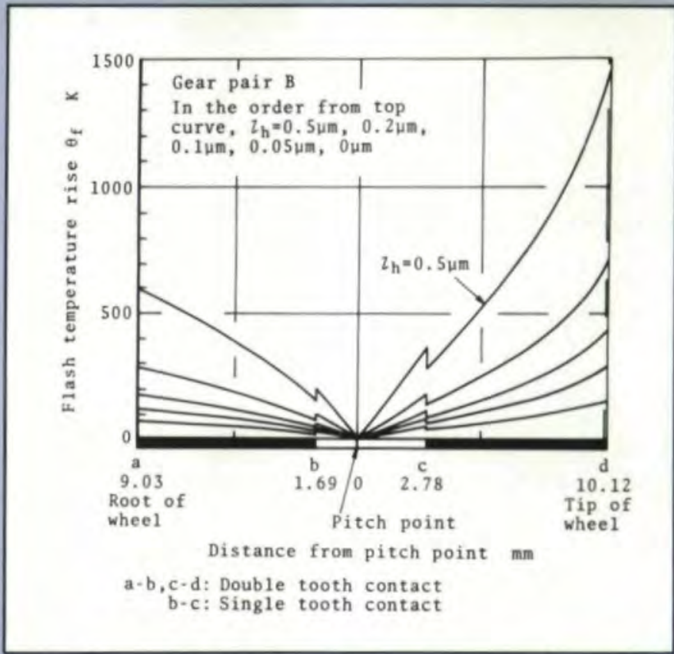

Fig. 11 – Variation in flash temperature rise at successive meshing positions along the line of action

of the gear tooth was exposed on the tooth surface.

Fig. 9 shows electron micrographs of the compo image and the *S-Kα* image which were obtained with a scanning X-ray microanalyzer at the tip of the gear tooth of the wheel with gear pair D. The MoS_2 film at the tip of the wheel was torn out due to wear, and the tooth surface was considerably smooth. However, the particles of sulfur were present at the tooth surface at which the scratching scar did not occur. From this photograph, it can be found the MoS_2 film is formed enough at the meshing faces at the incipience of surface failure by scoring, and the film significantly affects the scoring resistance of the gears.

Acceleration of Gear Box. Fig. 10 shows the variation in the acceleration due to oscillation of the gear box. The acceleration increased with an increasing test range. With gear pair D, the acceleration of the gear box suddenly increased by about 5g at P-1, and the incipience of surface failure by scoring could be detected by means of the measurement of the acceleration due to oscillation of the gear box.

Surface Temperature and Scoring Resistance. Fig. 11 shows the variation in the flash temperature rise at the successive meshing positions along the line of action, calculated by equations (1-5) under the following conditions: number of pinion teeth $z_1 = 18$, number of wheel teeth $z_2 = 40$, module $m = 4$ mm, face width $B_f = 7$ mm, backlash $S_n = 0.5$ mm, clearance coefficient $C_e = 0.25$, tooth load $P_n = 266$ N/mm, pinion speed $n_1 = 6000$ rpm.

The surface roughness at the meshing faces and the bulk-temperature of the gear teeth were assumed to be zero. The load-sharing was calculated from the elastic deformation of teeth. In this calculation, Young's modulus E and Poisson's ratio v of tooth material are assumed to be E = 206 GPa and $v = 0.3$, respectively. The coefficient of friction can be given by $\mu = 0.1\ V_p^{-0.2}$, where V_p is the peripheral velocity (m/s) at the pitch point.[5] Since the thickness of the MoS_2 film coated on the tooth surface is very small, it can be assumed that the mechanical properties of the MoS_2 film do not affect the band length of the Hertzian contact zone and the radius of relative curvature of the tooth surface at meshing position of the gears.

From this figure, it can be found that the flash temperature rise considerably increases with an increasing thickness of the MoS_2 film, and the effect of the MoS_2 film on the flash temperature rise is significant.

Fig. 12 shows the test range and the cumulative transmitted works per unit face width at the incipience of surface failure

Fig. 12 – Test range and cumulative transmitted works per unit face width at incipience of surface failure by scoring

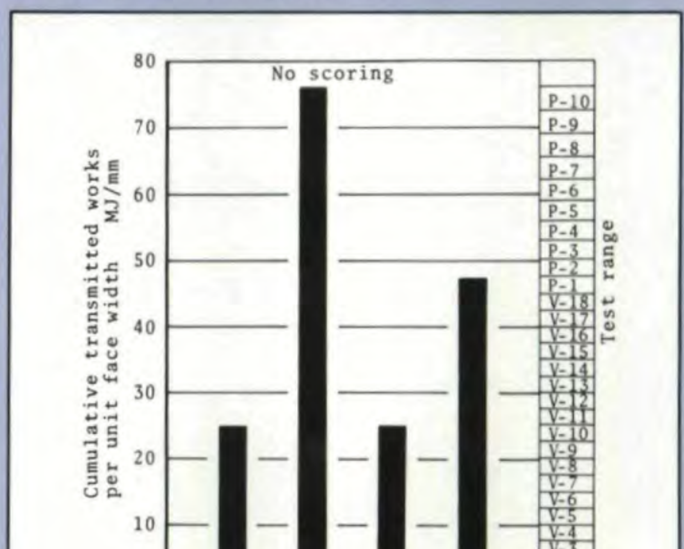

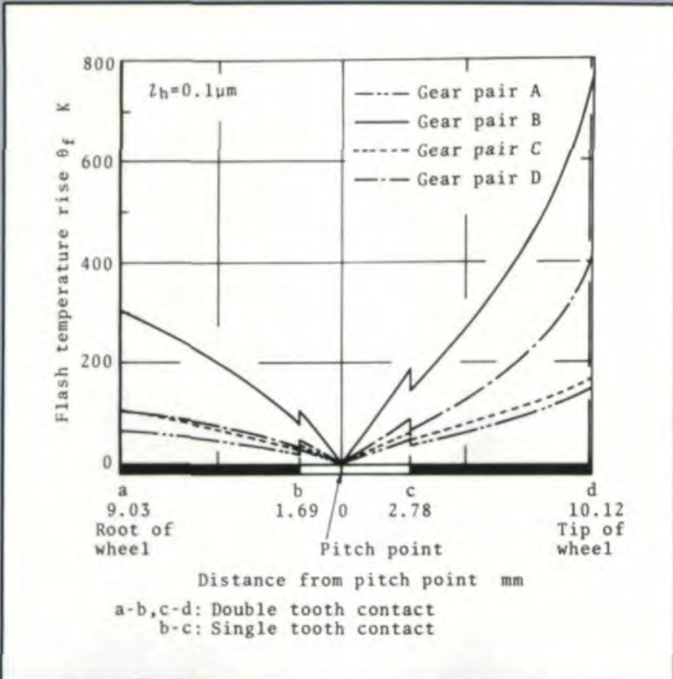

Fig. 13 – Variation in flash temperature rise at successive meshing positions along the line of action at incipience of surface failure by scoring

by scoring. With gear pair B, the tests were stopped at P-10 because the scoring resistance of the gears exceeds the load carrying capacity of the test machine. From this figure, it can be seen that gear pair B provides the highest scoring resistance of all test gears, and the MoS_2 film plays a significant role in increasing scoring resistance of the gears. Further, the scoring resistance of the gears with gear pair D is larger than that of the gears with gear pair C, and the MoS_2 film coated on the tooth surface of the wheel is more effective for the scoring resistance of the gears than that coated on the tooth surface of the pinion.

Fig. 13 shows the variation in the flash temperature rise at the successive meshing positions along the line of action at the incipience of surface failure by scoring. The flash temperature rise is calculated by substituting the tooth load, the pinion speed, the coefficient of friction and the thickness of the MoS_2 film into equations (1-5). From the observation of the sectional plane cut along the tooth profile, it was found that a part of the MoS_2 film was torn out due to wear and the thickness of the film was not uniform on the tooth surface. However, the thickness of the film was assumed to be $l_h = 0.1\ \mu m$.

From this figure, it is interesting to note that the maximum value of the flash temperature rise occurs at the meshing position where the tip of the wheel mates with the root of the pinion, and the position well agrees with the position at which destructive failure by scoring was observed.

The critical surface temperature for scoring of the gears is shown in Table 8. The critical surface temperature for scoring of the gears with gear pairs B and D is extremely high because the flash temperature rise of the gears is calculated under the assumptions that the MoS_2 film is uniformly distributed on the tooth surface and the coefficient of friction between the gear pairs coated with the MoS_2 film is equivalent to that between the gear pairs without it. However, a part of the MoS_2 film coated on the tooth surface was torn out just before surface failure was caused by scoring, and the thickness of the film was not uniform on the tooth surface. Further, according to the test results obtained with the four ball tests, the coefficient of friction between the balls coated with the MoS_2 film was smaller than that between the balls without it.

From the above cited facts, it can be considered that the critical surface temperature for scoring of the gears coated with the MoS_2 film is lower that the value shown in Table 8. However, the scoring resistance of the gears coated with the MoS_2 film is considerably large, and the MoS_2 film is considered to play a significant role in increasing scoring resistance of the gears.

Conclusions

Calculated surface temperatures and the experimental results obtained with four ball tests and gear tests with respect to the effect of the MoS_2 film on the scoring resistance of the gears are summarized as follows:

1. When the thickness of the surface layer is smaller than the band length of the Hertzian contact zone, the effect of the thermal properties in the surface layer on the flash temperature rise is significant, and the difference between the

Table 8 Critical surface temperature for scoring of gears

Gear pair	R_{rms} (a) μm	Bulk-temperature (b) θ_0 K	Maximum flash temperature rise θ_f K	Critical surface temperature (c) θ_{cr} K
A	0.33	340	148	540
B (d)	(0.37)	(351)	(770)	(1438)
C	0.36	337	167	570
D	0.48	346	411	1007

(a) R_{rms} is the mean value of the root mean square roughness along the tooth trace of the pinion and wheel just before scoring.
(b) θ_0 is the mean value of the bulk-temperature of the gear teeth of the pinion and wheel just before scoring.
(c) $\theta_{cr} = \theta_0 + \theta_f \times 1.27/(1.27 - R_{rms})$ [6]
(d) The numerals in parentheses are the value of the variables at P-10.

thermal properties in the surface layer and those in the core is an important problem.

2. Under comparatively low load (P<0.4 kN), the coefficient of friction between the balls coated with the MoS_2 film was 2/3 of that between the balls without it.

3. The scoring resistance of the gears coated with the MoS_2 film is considerably large, and the MoS_2 film plays a significant role in increasing scoring resistance of the gears. The development of the gears of which the load-carrying capacity against scoring is considerably large could be made.

References

1. BARTZ, W. J., "Some Investigations on the Influence of Particle Size on the Lubricating Effectiveness of Molybdenum Disulfide," *ASLE Trans.*, Vol. 15, 1972, pp. 207-215.
2. TERAUCHI, Y., MIYAO, Y., and NADANO, H., "On the Flash Temperature Rise of the Tooth Surface of Surface-Hardened Gears," *Bulletin of the JSME*, Vol. 16, No. 99, 1973, pp. 1443-1456.
3. YAMAMOTO, T., and HANADA, H., "Manufacturing Process of Solid Lubricants," *Jour. Japan Soc. Lub., Engrs.* (in Japanese), Vol. 27, No. 4, 1982, pp. 233-237.
4. WELLAUER, E. J., and HOLLOWAY, G. A., "Application of EHD Oil Film Theory to Industrial Gear Drives," ASME *Journal of Engineering for Industry*, Vol. 98, No. 2, May 1976, pp. 626-634.
5. *ISO TC60/WG6*, "Calculation of Scoring Resistance," Dutch-Swiss draft, May 1977.
6. TERAUCHI, Y., and NADANO, H., "Effect of Tooth Profile Modification on the Scoring Resistance of Spur Gears," *Wear*, Vol. 80, 1982, pp. 27-41.

This article was presented previously at the ASME Design Engineering Conference, October 1984. Paper No. 84-DET-59.

TECHNICAL CALENDAR

October 5-8, 1986
AGMA Fall Technical Conference & Gearing Exhibit
Hyatt Regency Chicago in Chicago, IL

AGMA's Fall Technical Meeting will provide a forum for discussion of the design and manufacture of gears, flexible couplings and mechanical power transmission products. This year there will be an exhibit of gear generating machinery, gear design hardware and software, as well as other products of use to the industry.

For further information contact:
Rich Norment or Wendy Allen at (703) 684-0211.

September 17-19, 1986
Ohio State University Gear Noise Seminar
Columbus, OH

The three-day course will cover general noise measurements and analysis, causes of gear noise, gear noise reduction techniques, dynamic modeling, gear noise signal analysis, and modal analysis of gear boxes.

For further information contact:
Mr. Richard Frasher at (614) 422-8143.

November 11-13, 1986
SME Gear Processing and Manufacturing Clinic
Chicago, IL

Call for Papers: The Society of Manufacturing Engineers has issued a call for papers for this meeting. Please submit all papers on or before July 15th. The clinic will also include vendor tabletop
exhibits.

For more information, contact Joseph A. Franchini
at SME (313) 271-1500, ext. 394.

November 19-21, 1986
Seminar: Gear System Design for Minimum Noise
University of Wisconsin

This course provides an overview of noise control in gear sysem design and offers practical design information with a minimum of acoustical theory. The course is for engineers who design or specify gears or gear drives.

For additional information contact:
John Leaman at (414) 224-4189.

ENGINEERING CONSTANTS . . .

COMMONLY USED ENGINEERING CONSTANTS

Below are listed a variety of commonly used constants arranged numerically to permit ease of reference. Wherever an asterisk (*) is shown, the constant is exact as given, it being generally a mathematical constant or one fixed by definition. In cases where the first constant listed is followed by another in parenthesis, the first is the round number generally used, while the second is the more exact value.

0* deg. C. = freezing point of water.

1 = atomic wgt. hydrogen.

100* deg. C. = boiling point of water at atm. press.

10.764* sq.ft. = 1 sq. meter.

0.1134 hp. = available water power from 1 cu.ft.-sec. falling 1 ft.

1.134 ft. water at 62 deg. F. = 1 in. Hg. at 62 deg. F.

1,150.4 B.t.u. = Total heat sat. steam at atm. press.

11.52 lb. = theoret. air to burn 1 lb. carbon.

12 = atomic wgt. carbon (C).

12.387 cu.ft. = vol. 1 lb. air at 32 deg. F. and 14.7 lb. per sq.in.

12.52 lb. = wgt. theoret. combustion products from 1 lb. C.

1,273,239* circular mils = 1 sq.in.

13.144 cu.ft. = vol. 1 lb. air at 62 deg. F. and 14.7 lb. per sq.in.

1.3410 hp. = 1 kw.

14 = atomic wgt. nitrogen (N).

1.406 = V = ratio of Cp to Cv for air.

1.4142* = square root of 2.

14.223* lb. per sq.in. = 1 kg. per sq.cm. = 1 "metric atmosphere".

144* sq.in. = 1 sq.ft.

144 (143.15) B.t.u. = latent heat of fushion of ice.

14,600 B.t.u. per lb. = Cal. val. of carbon (C).

14.7 (14.696*) lb. per sq.in. = atm. press.

16* ounces = 1 lb.

16 = atomic wgt. oxygen (O).

0.1689 = Cv for air.

0.017138* grammes per litre = 1 grain per gal.

17.138* ppm = 1 grain per gal.

1.728* cu.in. = 1 cu.ft.

1.7321* = square root of 3.

1.8* B.t.u. per lb. = 1 kg. calorie per kg.

1.8* Fahrenheit degrees = 1 Centigrade degree.

18 = mol. wgt. water (H_2O).

2,000* lb. = 1 short ton.

2.0355 in. Hg. at 32 deg. F. = 1 lb. per sq.in.

2.0416 in. Hg. at 62 deg. F. = 1 lb. per sq.in.

2,116.3* lb. per sq.ft. = atm. press.

212* deg. F. = boiling point water at atm. press.

2.2046 lb.* = 1 kg.

223.8* × sq. root adiabatic heat drop = theoret. vel., ft. per sec., of steam expanding through nozzle.

2,240* lb. = long ton.

2.3026* × $\log_{10}a$ = $\log_e a$.

2.309 ft. water at 62 deg. F. = 1 lb. per sq.in.

231* cu.in. = 1 gal.

0.2375 = Cp for air.

2.54* cm. = 1 in.

2,545 (2,547) B.t.u. per hr. = 1 hp.

2.666 lb. = wgt. oxygen required to burn 1 lb. carbon.

27* cu.ft. = 1 cubic yard.

−270 deg. C. = absolute zero.

2.7183* = e = base hyperbolic logs.

27.71 in. water at 62 deg. F. = 1 lb. per sq.in.

277.274 cu.in. = 1 British gal.

28 = mol. wgt. nitrogen gas (N_2).

28 = mol. wgt. carbon monoxide (CO).

28.8 = equivalent mol. wgt. of air.

288,000* B.t.u. per 24 hr. = 1 ton of refrigeration.

29.921* in. Hg. at 32 deg. F. = atm. press.

3* ft. = 1 yard.

30 in. Hg. at 62 deg. = atm. press. (very closely).

3.1416* = π (Greek letter "pi") = ratio circumference of circle to diameter = ratio area of circle to square of radius.

32* deg. F. = freezing point of water = 0 deg. C.

32 = atomic wgt. sulphur (S).

32 = mol. wgt. oxygen gas (O_2).

32.5* gal. = 1 barrel.

3.2808* ft. = 1 meter.

33,000* ft.-lb. per min. = 1 hp.

33.947 ft. water at 62 deg. F. = atm. press.

3,415 B.t.u. = 1 kw.-hr.

3.45* lb. steam "f. & a. 212" per sq.ft. per hr. = rated boiler evaporation.

34.56 lb. = wgt. air to burn 1 lb. hydrogen (H).

35.314* cu.ft. = 1 cu. meter.

3.785* liters = 1 gal.

39.37* in. = 1 meter = 100 cm.

3.9683* B.t.u. = 1 kg. calorie.

4,000 B.t.u. (4,050) = cal. val. of sulphur (S).

4.32 lb. = wgt. air req. to burn 1 lb. sulphur (S).

0.433 lb. per sq.in. = 1 ft. of water at 62 deg. F.

44 = mol. wgt. carbon dioxide (CO_2).

0.45359* kg. = 1 lb.

−460 (459.6) deg. F. = absolute zero.

0.47 B.t.u. per pound per deg. F. = approx. specific heat of superheated steam at atm. press.

0.491 lb. per sq.in. = 1 in. Hg. at 62 deg. F.

5.196 lb. per sq.ft. = 1 in. water at 62 deg. F.

5,280* ft. = 1 mile.

53.32 = R, for air, in equation: $PV = MRT$.

550* ft.-lb. per sec. = 1 hp.

57.296* deg. = 1 radian (angle).

58.349* grains per gal. = 1 gram per liter.

59.76 lb. = wgt. 1 cu.ft. water at 212 deg. F.

61.023* cu.in. = 1 liter.

62,000 B.t.u. = cal. val. (higher) hydrogen (H).

0.62137* miles = 1 kilometer.

0.062428* lb. per cu.ft. = 1 kg. per cu. meter.

62.5 (62.355) lb. = wgt. 1 cu.ft. water at 62 deg. F.

7,000* grains = 1 lb.

0.0735 in. Hg. at 62 deg. F. = 1 in. water at 62 deg. F.

746 (745.7) watts = 1 hp.

7.5 (7.4805*) gal. = 1 cu.ft.

760* millimeters Hg. = atm. press. at 0 deg. C.

0.07608 lb. = wgt. 1 cu.ft. air at 62 deg. F. and 14.7 lb. per sq.in.

778 (777.5) ft.-lb. = 1 B.t.u.

0.7854* (= 3.1416 ÷ 4) × diameter squared = area circle.

8 = lb. oxygen required to burn 1 lb. hydrogen (H).

8.025* (= square root of $2g$) × square root of head (ft.) = theoretical velocity, ft. per sec.

0.08073 lb. = wgt. 1 cu.ft. air at 32 deg. and 14.7 lb. per sq.in.

8⅓ (8.3356) lb. = wgt. 1 gal. water at 62 deg. F.

8,760* hr. = 1 year of 365 days.

88* ft. per sec. (min.) = 1 mile per min. (hr.).

9* sq.ft. = 1 sq.yd.

0.0929* sq. meters = 1 sq.ft.

970.4 B.t.u. = Latent heat of evap. of water at 212 deg. F.

FORMULAS FOR DETERMINING GEAR DIMENSIONS BY METRIC PITCH

Module is the pitch diameter in millimetres divided by the number of teeth in the gear. Pitch diameter in millimetres is the Module multiplied by the number of teeth in the gear.

M = Module.
D′ = The pitch diameter of gear in millimetres.
D = The whole diameter of gear in millimetres.
N = The number of teeth in gear.
D″ = The working depth of teeth.
t = Thickness of teeth on pitch line.
f = Amount added to depth for clearance.
D.P. = Diametral Pitch

Then

$$M = \frac{D'}{N} \text{ or } \frac{D}{N+2}$$

$$D' = NM.$$

$$D = (N+2)\ M.$$

$$N = \frac{D'}{M} \text{ or } \frac{D}{M} - 2$$

$$D'' = 2\ M.$$

$$t = M\ 1.5708.$$

$$f = \frac{M\ 1.5708}{10} = .157\ M.$$

$$M = \frac{25.4}{D.P.}$$

$$D.P. = \frac{25.4}{M}$$

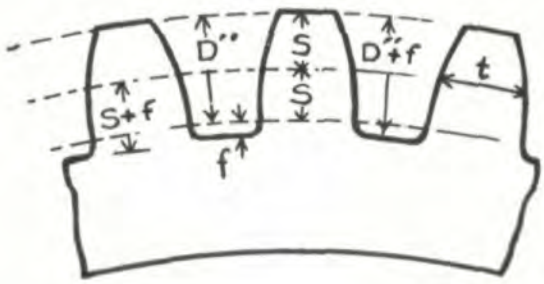

The Module is equal to the part marked "S" in diagram, measured in millimetres and parts of millimetres.

Pitches Commonly Used—Module in Millimetres

Module	Corresponding English Diametral Pitch
½ mm.	50.800
¾	33.867
1	25.400
1.25	20.320
1.5	16.933
1.75	14.514
2	12.700
2.25	11.288
2.5	10.160
2.75	9.236
3	8.466
3.5	7.257
4	6.350
4.5	5.644
5	5.080
5.5	4.618
6	4.233
7	3.628
8	3.175
9	2.822
10	2.540
11	2.309
12	2.117
13	1.954
14	1.814
15	1.693
16	1.587

CONVERTING METRIC INTO INCHES

Millimetres × .03937 = inches.
Millimetres ÷ 25.4 = inches.
Centimetres × .3937 = inches.
Centimetres ÷ 2.54 = inches.
Metres × 39.37 = inches. (Act Congress).
Metres × 3.281 = feet.
Metres × 1.094 = yards.
Kilometres × .621 = miles.
Kilometres ÷ 1.6093 = miles.
Kilometres × 3280.87 = feet.
Square Millimetres × .00155 = square inches.
Square Millimetres ÷ 645.16 = square inches.
Square Centimetres × .155 = square inches.
Square Centimetres ÷ 6.451 = square inches.
Square metres × 10.764 = square feet.
Square Kilometres × 247.1 = acres.
Hectare × 2.471 = acres.
Cubic Centimetres ÷ 16.383 = cubic inches.
Cubic Centimetres ÷ 3.69 = Fl. drachms (U.S. Phar.)
Cubic Centimetres ÷ 29.57 = Fl. ounces (U.S. Phar.)
Cubic Metres × 35.315 = cubic feet.
Cubic Metres × 1.308 = cubic yards.
Cubic Metres × 264.2 = gallons (231 cubic inches).
Litres × 61.022 = cubic inches (Act Congress).
Litres × 33.84 = fluid ounce (U.S. Phar.).
Litres × .2642 = gallons (231 cubic inches).
Litres ÷ 3.78 = gallons (231 cubic inches).
Litres ÷ 28.316 = cubic feet.
Hectolitres × 3.531 = cubic feet.
Hectolitres × 2.84 = bushels (2150.42 cubic inches).
Hectolitres × .131 = cubic yards.
Hectolitres ÷ 26.42 = gallon (231 cubic inches).
Grammes × 15.432 = grains (Act Congress).
Grammes ÷ 981 = dynes.
Grammes (water) ÷ 29.57 = fluid ounce.
Grammes ÷ 28.35 = ounce avoirdupois.
Grammes per cubic cent. ÷ 27.7 = lbs. per cu. inch.
Joule × .7373 = foot pounds.
Kilo-grammes × 2.2046 = pounds.
Kilo-grammes × 35.3 = ounces avoirdupois.
Kilo-grammes ÷ 907.18581 = tons (2000 lbs.) or × .00110231.
Kilo-grammes per sq. cent. × 14.223 = lbs. per sq. in.
Kilo-gram-metres × 7.233 = foot pounds.
Kilo per Metre × .672 = pounds per foot.
Kilo per Cubic Metre × .026 = pounds per cubic ft.
Kilo per Cheval × 2.235 = pounds per H.P.
Kilo-Watts × 1.34 = Horse-Power.
Watts ÷ 746 = Horse-Power.
Watts ÷ .7373 = foot pounds per second.
Calorie × 3.968 = B.T.U.
Cheval Vapeur × .9863 = Horse-Power.
(Centigrade × 1.8) + 32 = degree Fahr.
Gravity Paris = 980.94 centimetres per second.

BACK TO BASICS...

Bevel Gear Development and Testing Procedure

The Gleason Works
Rochester, New York

The most conclusive test of bevel and hypoid gears is their operation under normal running conditions in their final mountings. Testing not only maintains quality and uniformity during manufacture, but also determines if the gears will be satisfactory for their intended applications.

Gears are checked in the testing machine for the following conditions: tooth size in relation to a master, or to the mating member, mounting distance of gear and pinion, the position of the tooth contact, the quality of the surface finish, the amount of TOPREM®, the amount of clearance, visual eccentricity, tooth spacing errors, and the general running qualities of the gear and pinion, as well as the axial displacement tolerances of the gear set. Gears are also checked for bias and profile on the test machine.

Definitions

It is important that certain terms be defined before any testing and development procedure for bevel gears is presented. (Fig. 1)

Gear – of two gears that run together, the one with the larger number of teeth is called the gear. It is the driven member of a pair of gears.

Pinion – the member with the smaller number of teeth. With miter gears it is the driving member.

Toe – the portion of the tooth surface at the inner end.

Heel – the portion of the tooth surface at the outer end.

Top – the upper portion of the tooth surface.

Flank – the lower portion of the tooth surface.

Top Land – the non-contacting surface at the top of the tooth.

Root Land – the non-contacting surface at the bottom of a tooth space.

Top Side and Bottom Side – in conventional machines for producing both straight and curved tooth bevel gears, the cutter or cutting tools always operate on the left hand side of the gear blank as viewed from the front. The term *top* refers to the upper side of the tooth in this position, and the term *bottom* refers to the lower side.

Top Side of Tooth
Left hand spiral – convex side of tooth.
Right hand spiral – concave side of tooth.

Bottom Side of Tooth
Left hand spiral – concave side of tooth.
Right hand spiral – convex side of tooth.

The terms *bottom side* or *top side* would always apply to a specific side, regardless of the hand of spiral, and also with straight bevel gears. When the *forward* side in the testing machine is running, the rotation of the pinion spindle is clockwise when viewed from the source of power, and the *bottom side* of the pinion will contact the *bottom* side of the gear. When the pinion is running in the *reverse* direction, the rotation is counter-clockwise, and the *top side* of the pinion will contact the *top side* of the gear. It would, therefore, be better to refer to *bottom side* or *forward side*, and *top side* or *reverse side*.

When referring to a specific side of the tooth, the terms *drive side* or *coast side* are quite often used, but, unless a full knowledge of the application is available, these terms

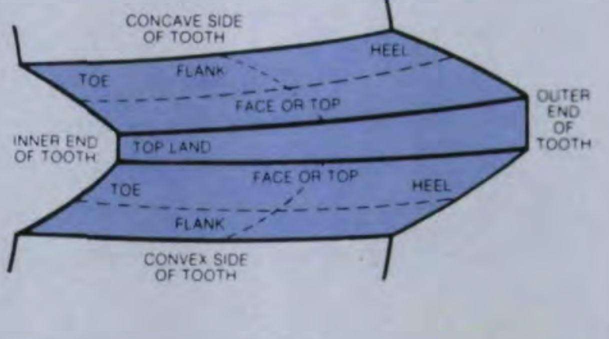

Fig. 1

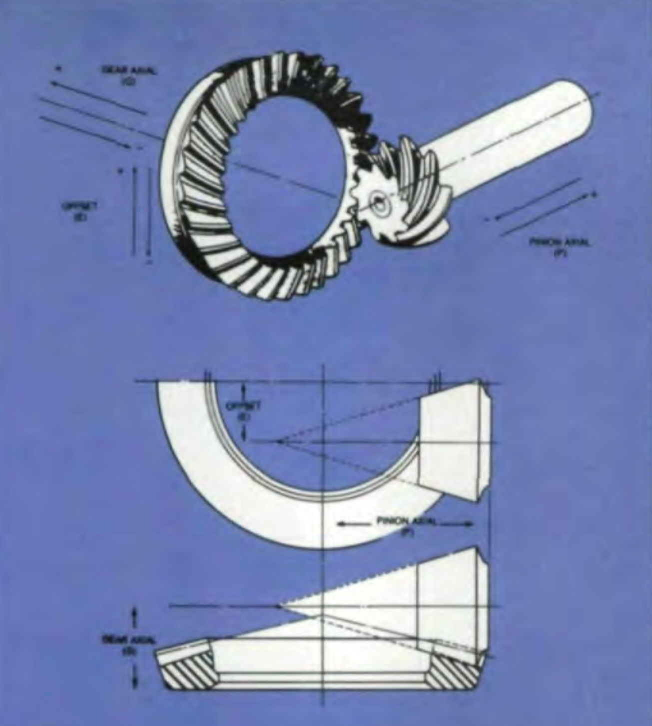

Fig. 2

would not be specific. Normally the concave side of the pinion is called the *drive side* and the convex side of the pinion is called the *coast side*, but in many cases either side may drive. Also, with straight bevel gears, there is no concave or convex side, so it again would be difficult to correctly specify by *drive side* or *coast side*.

Right Hand Spiral – when viewed from the front, above center, the spiral angle of a bevel gear curves to the right.

Left Hand Spiral – when viewed from the front, above center, the spiral angle of a bevel gear curves to the left.

Clockwise Rotation – the pinion rotates clockwise when viewed from the back.

Counter-clockwise Rotation – the gear rotates counter-clockwise when viewed from the back.

Tooth Contact – the summation of all instantaneous lines of contact on a tooth surface. Also, the area on a tooth surface from which marking compound is removed when the gears are run together in a test machine.

EPG

Tooth contact of mating gear teeth can be positioned by manipulation of tester machine adjustments. The directions of these movements and their designating letters are shown in Fig. 2. This sketch is of a hypoid pair, but the directions of the movements are equally applicable to spiral, or straight bevel gears.

(E) = movement perpendicular to the gear and pinion axes. A change in offset (E) can be made by moving the pinion relative to the gear. Or, it can be made by moving the gear relative to the pinion, depending upon the design of the testing equipment used.

(P) = pinion axial movement. A change in the pinion axial distance (P) can be made by moving the pinion relative to the gear. Or, it can be made by moving the gear relative to the pinion, depending upon the design of the testing equipment used. (P) is commonly known as a pinion cone change or a pinion mounting distance change.

(G) = gear axial movement. A change in the gear axial distance (G) can be made by moving the pinion relative to the gear. Or, it can be made by moving the gear relative to the pinion, depending upon the design of the testing equipment used. (G) is commonly known as a backlash change, a gear cone change or a gear mounting distance change.

EPG Sign Conventions

The readings on all dials on testing machine E, P and G adjustments should be considered "zero" readings, when the gears are mounted at the mounting distances and hypoid offset specified on the Summary.

(E+) indicates an increase in offset.
(E−) indicates a decrease in offset.
(P+) indicates an increase in pinion axial distance.
(P−) indicates a decrease in pinion axial distance.
(G+) indicates an increase in gear axial distance.
(G−) indicates a decrease in gear axial distance.

V & H

The E & P check accomplishes the same thing as the former V & H check. "V" is equivalent to (E) and "H" is equivalent to (P).

Testing Procedures

A. The E & P Check

The E & P (offset and pinion axial) check is used as a method of measuring the axial displacement movement required in the test machine, to move the contact from a *central profile contact shading out at the toe to a central profile* contact shading out at the heel.

The following can be determined by analysis of the E & P check:

1. The total length of contact.
2. The amount and the direction of bias (bias in or bias out).
3. Position of the tooth contact in relation to correct testing machine centers.
4. By visual observation of the tooth contact, when the heel and the toe E & P checks are on the tooth at the same time, the relative length of the heel and toe contact is determined and the width of profile can be observed.
5. The approximate amount of displacement that the gear will withstand without causing load concentration.

E & P Check (Left Hand Spiral Pinion)

Increase the gear offset and decrease the pinion axial distance to move the contact to the toe on the concave side of the pinion or to the heel on the convex side of the pinion.

When moving the contact to the heel on the concave side of the pinion or to the toe on the convex side of the pinion, the gear offset is decreased and the pinion axial distance is increased.

E & P Check (Right Hand Spiral Pinion)

To move the contact to the toe on the convex side of the pinion or to the heel on the concave side of the pinion, the gear offset is increased, and the pinion axial distance is increased. To move the contact to the heel on the convex side of the pinion or toe on the concave side of the pinion, the gear offset and the pinion axial distance are decreased.

E & P Example:

TOE	HEEL	TOTAL
E +3	E −13	16
P −2	P +12	14

The preceding example refers to the *bottom side* because decreasing the offset of the gear in relation to the pinion (E−) will always move the contact toward the *bottom heel* position. (If the heel value was E +13, the reference would be to the top heel position and the offset of the gear would be increased in relation to the pinion).

A *Bias In* contact is indicated in the previous E & P example because the **total** offset value is greater than the total pinion axial value. In a *Bias Out* contact the total offset value is less than the total pinion axial value. The example also illustrates that the contact would be near the toe, in the center of the tooth profile, and would have a slight *bias in* direction.

L.H. Pinion

Concave Side			Convex Side		
TOE	HEEL	TOTAL	TOE	HEEL	TOTAL
E(+)	E(−)	—	E(−)	E(+)	—
P(−)	P(+)		P(+)	P(−)	

R.H. Pinion

Concave Side			Convex Side		
TOE	HEEL	TOTAL	TOE	HEEL	TOTAL
E(−)	E(+)	—	E(+)	E(−)	—
P(−)	P(+)		P(+)	P(−)	

B. Adjusting Gear Centers for Development

It is recommended that extra pinion blanks be made available for development purposes. One of these should have teeth cut to *finish* size for the first test. When testing the tooth contact between the gear and the pinion teeth, the gear is set to its correct mounting distance and held in this position throughout the development.

1. As the pinion tooth thickness is reduced, the backlash will increase, without affecting the nature of the tooth contact. This holds true only if the base on the gear cutting machine has not been adjusted during development.
2. On right-angle test machines, this is done by keeping the pinion cone stationary. On universal testers the gear cone is kept in a fixed position.

If no extra pinions are available, the development must be made on pinions which are not cut to finish tooth size. This is done by increasing the testing machine mounting distances on both members by moving the gear and pinion cone out until the desired amount of backlash is obtained. *The gear and pinion cone must be moved out in proportion to the numbers of teeth in the two members.*

Example #1:

20 x 40 combination – 90° shaft angle – Opening in proportion to the ratio being tested would give a .002" increase on the gear cone for every .001" increase on the pinion cone.

Example #2:

10 x 30 combination – 90° shaft angle – Increasing the testing machine mounting distances in proportion to the ratio being tested would give a .003" increase on the gear cone for every .001" increase on the pinion cone.

On universal test machines (arranged to test gears at any shaft angle), the method for increasing the mounting distances is controlled by the formula below.

X_G = amount to increase gear axial distance (G+)

X_P = amount to increase pinion axial distance (P+)

$$X_P = X_G \left[\frac{\text{cosine of gear pitch angle}}{\text{cosine of pinion pitch angle}} \right]$$

Example:

21 x 25 combination, 142° shaft angle –
Gear Pitch Angle = 85°10′; cosine = 0.0843
Pinion Pitch Angle = 56°50′; cosine = 0.5471
If the gear axial is moved *out* 0.013", the pinion axial

must be moved *out* $0.013'' \times \frac{0.0843}{0.5471} = 0.002''$.

If the pitch angle exceeds 90° (internal gear), the cosine of the gear pitch angle will be negative, causing the pinion axial to be moved *in* and the gear axial to be moved *out*.

3. Running at increased mounting distances, the gears will show a contact similar to that which they will have when cut to size, only it will be nearer the heel of the tooth. *The final check should be made with both the gear and pinion at their specified mounting distances and backlash.*

Checking Backlash

The term backlash, used in these instructions, refers to normal backlash (backlash in a direction perpendicular to the tooth surface). To obtain backlash in the plane of rotation, the (normal) backlash must be divided by the cosine of the spiral angle times the cosine of the pressure angle.

Bevel gears are cut to have a definite amount of backlash which varies according to the pitch and operating conditions. This backlash is necessary for the safe and proper running of the gears. If there is insufficient backlash, the gears will

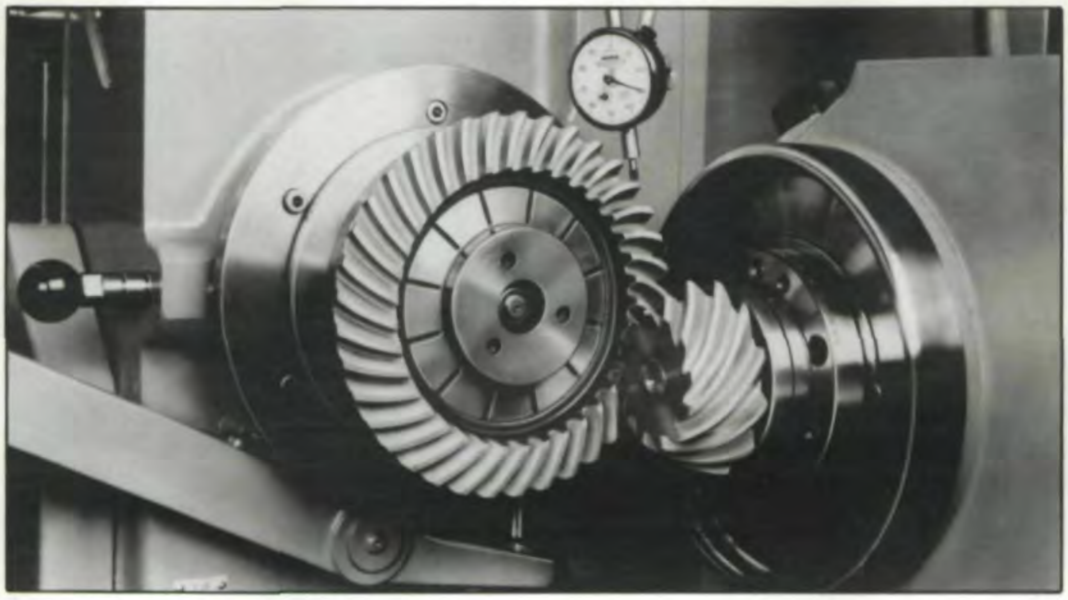

Fig. 3

be noisy, wear excessively, and possibly score on the tooth surfaces, or even break. In production testing, backlash measurement is used as a gage of tooth thickness.

Backlash should be measured at the tightest point of mesh with the gears mounted on their correct centers. To make this measurement on the testing machine, hold the pinion solidly against rotation, rigidly mount a dial indicator against a gear tooth being sure that the indicator stem is perpendicular to the tooth surface at the extreme heel. (See Fig. 3.) The backlash will then be shown by the indicator when the gear is turned back and forth by hand.

Backlash variation is measured by locating the points of maximum and minimum backlash in the pair gears and obtaining the difference. For precision gears this variation, in general, should not exceed 0.001".

After checking backlash by the above method on the finally approved pair of gears, the production control of backlash may be checked more easily by the following method:

The approved pair of gears (control gears) are mounted in the testing machine on their correct centers. The gear is then moved axially into metal-to-metal contact with the pinion. The amount of movement from its initial position is observed. Then, when testing the production gears, move past the correct centers by this same amount.

The axial movement of the gear for 0.001" change in backlash varies with the pressure angle approximately as follows:

Pressure Angle	14½°	20°	25°
Axial Movement of Gear	0.002"	0.0015"	0.001"

The following table gives the recommended backlash for gears assembled ready to run. Backlash for pitches, other than those listed, may be obtained by interpolation.

TABLE OF BACKLASH

Diametral Pitch	Backlash
1	0.020" to 0.030"
2	0.012" to 0.016"
3	0.008" to 0.011"
4	0.006" to 0.008"
6	0.004" to 0.006"
10	0.002" to 0.004"
20 and finer	0.001" to 0.003"

In certain applications, the backlash tolerance may have to be altered to meet specific requirements.

Procedure for Checking the Amount of TOPREM®

TOPREM is a decrease in the pressure angle at the tip of the cutter blades. This decrease in pressure angle causes more stock to be removed in the fillet of the tooth when the blades cut. TOPREM is usually applied to the pinion member to prevent interferences at the top of the gear tooth during lapping.

Use a dummy pinion that has been cut to the correct tooth depth, small in tooth size, and developed to a full profile contact. Run the gear and pinion together at the correct theoretical mounting distances and note the distance between the top edge of the contact and the top edge of the tooth. This is the amount of effective TOPREM.

To measure the amount of effective TOPREM, the following sequence should be followed:

Increase the gear axial distance +.010" and run the gears.

If the contact is not to the top edge of the gear tooth, increase the gear axial distance +.010", check again, and if necessary, increase the gear axial distance at increments of .010", until the contact is just to the top edge of the gear tooth. The amount of increase in the gear axial distance, from the theoretical mounting distance, is the amount of effective TOPREM. The normal amount of effective TOPREM is between .025" and .035".

NOTE:

If, after following the above procedure, the check shows that additional TOPREM is required, use a cutter that has been ground to give a greater amount of TOPREM. This should be done before changing the depth of the tooth slot because of a possible interference in the root.

If less than .025" effective TOPREM is noted, recut the pinion with the depth decreased by .010". Check the pinion and gear with the gear axial distance decreased to -.030" or -.035" and rotate the gear and pinion slowly. Look for interference at the pinion root radius. If no interference is noted, the pinions may be cut at the decreased depth. This will give the maximum amount of effective TOPREM that has been ground onto the cutter.

Procedure for Soft Testing

1. Have a pinion cut small enough to permit running it with a mating gear at correct mounting distances for both the gear and pinion.
2. With the gears properly installed in the test machine, carefully jog the machine and apply a suitable marking compound to the teeth. Run the machine carefully without any brake load, noting the position of the tooth contact. If the contact is too far out of position, any further amount of running could damage the tooth surfaces.
3. Adjust the test machine, if necessary, to obtain a central toe contact with central profile. The amount of offset and pinion axial movement required to properly position the contact should be recorded. This information is used in making the corrective changes on the cutting machine. Recut the pinion. The tooth contact should be in proper position before making an E & P check.
4. Check the gears for E & P and record the values. Observe center, heel and toe contacts for width of profile, bias contact, fillet interference and TOPREM. Also make sure that they are finish cut completely to the ends of the teeth (rolled out in cutting).
5. Set the test machine to the *Average Contact* values and note the lengthwise positioning of the contact on the tooth. If the contact is closer to the heel, this will show that the heel portion of the contact is longer than the toe portion.
6. When the final positioning of the contact has been made in cutting, the gears must be checked for the following:
   a. Whole depth of both pinion and gear.
   b. Fins or steps in the root of both pinion and gear.
   c. Interference at radii of both pinion and gear.
   d. Surface finish on both pinion and gear.
   e. Amount of effective TOPREM.
   f. Possible tooth defects and visual eccentricity.
   g. Length of contact at toe and heel checks.
   h. Final E & P check for length of contact and proper bias.
   i. Profile adjustment and sound at toe, center, and heel.
7. When a production piece is finish cut on one side, it is important that enough stock be left to completely clean up the remaining side when it is finish cut to the proper backlash at the correct mounting distances for both pinion and gear.

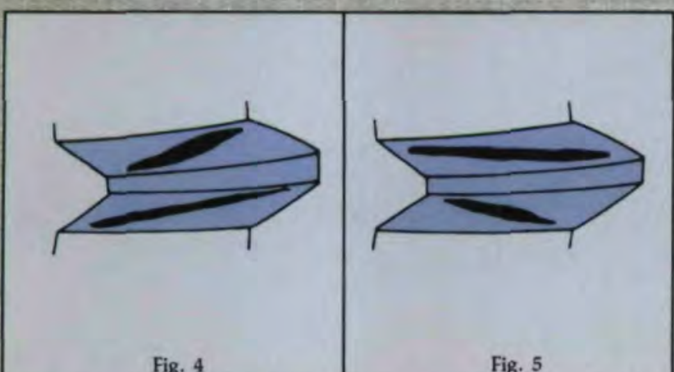

Fig. 4 Fig. 5

Hardening-Effects on the Tooth Contact

When gears are hardened, the spiral teeth have a tendency to straighten. Since this condition applies to both the gear and the pinion, the effect is not extreme when the two hardened members are run together. Although the pinion is likely to change more than the gear, in hypoids, due to having a longer face and higher spiral angle, compensating position changes can be allowed in cutting to maintain a correct position and bias after hardening.

Since *bias in* is introduced in hardening, it is usually desirable to have a slight amount of *bias out* in soft gears. Also due to the straightening tendency of the spiral teeth, it is sometimes necessary to have the contact central on the concave side of the pinion and favoring the toe on the convex side of the pinion.

The amount of change can only be determined by trial, but generally the length of the contact will show approximately one-third less E & P movement and the profile will normally change from a full width profile to a narrower profile. This will produce a satisfactory contact with a normal amount of adjustment.

The contact on the convex side of the pinion will also be higher after hardening, therefore, it may be desirable to have the contact deeper on the convex side of the soft pinion to compensate for that change.

Conditions That Can Be Determined by a Test Machine

1. Bias in and Bias Out

Bias In (Fig. 4)

The total *offset value* in the E & P check is greater than the total pinion axial value.

A visual check of *bias in* can be made as follows:

The contact is diagonal to the pitch line, and on the con-

NOW A NEW HOBBER FROM MITSUBISHI, YOU CAN'T BEAT IT! COMPARE AND SEE!

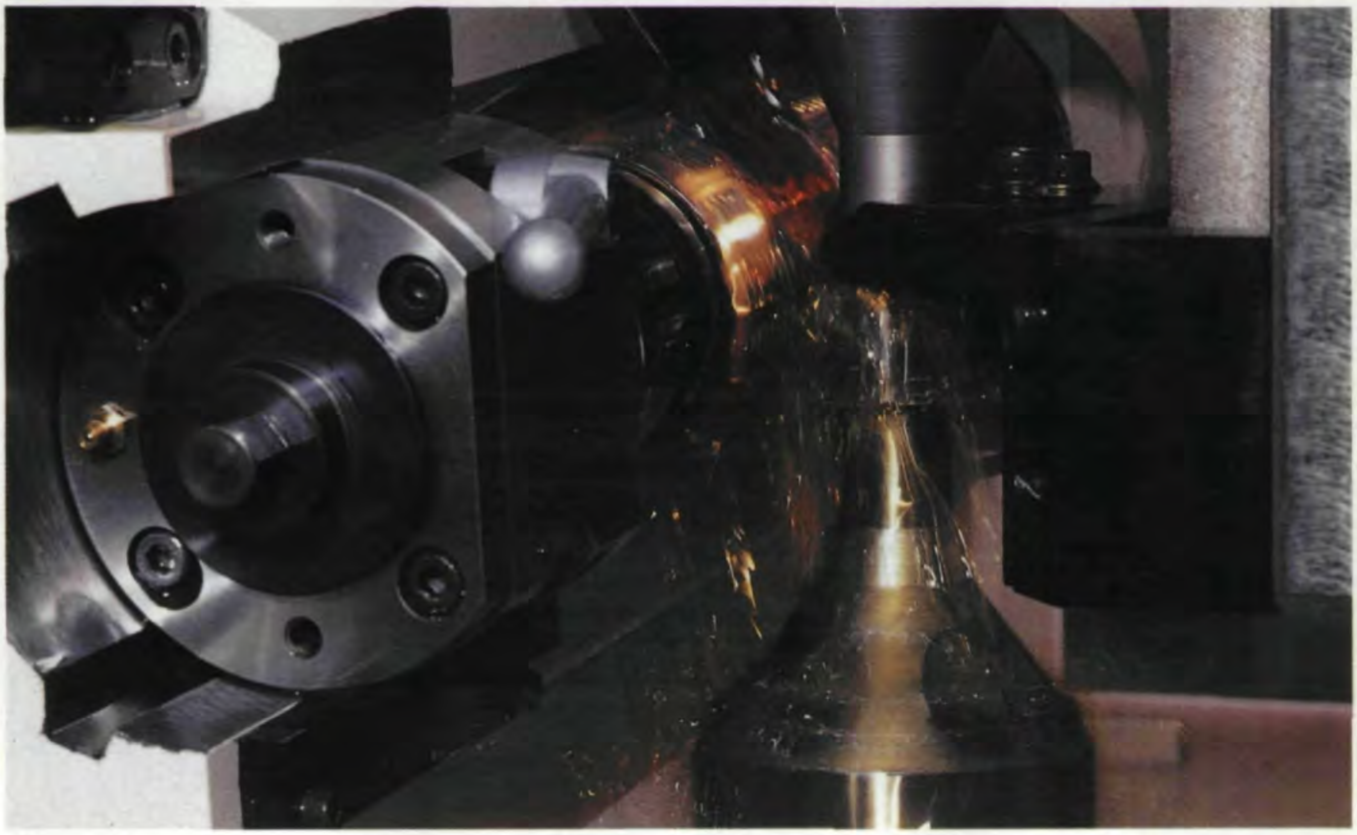

In addition to the GA-series CNC gear hobbing machines which covers a range from 10″ to 40″ diameter gears, Mitsubishi is now announcing the new high performance GA15CNC gear hobber. The GA15CNC is a 6″ machine with hob rotation of 1000rpm and table rotation of 150rpm as standard where it is an option with other manufacturers. This enables you to use multiple thread hobs to get higher production rates. Our results show that the cutting time can be reduced to about one half of the conventional machines. Needless to say, with the CNC control feature, there are no gears to change. Quick change hobs and quick change fixtures all adds up to quick changeover time. Setup time is reduced to about one third compared to conventional machines. "MENU" programming is another great feature. This relieves the operator from tedious calculations. Just input the gear and hob data. The built-in software will do all the calculations for you! You can also save floor space, hence money, with our machine. It takes only 50 sq. ft. of floor space! Compare it with the others. You'll be saving 1/2 to 3/4 of your valuable floor space! This is only the beginning! For further details, call or write us NOW!

Main Specifications

Maximum part diameter	6″, optional 8″
Maximum pitch	6DP
Maximum hob diameter	4.7″
Maximum hob length	7″
Hob shift	5″
Hob speed	150 to 1000 rpm
Hob head swivel	+/−45 deg.
Table speed	150 rpm
Main motor	7.5 hp

CNC GEAR HOBBER

MITSUBISHI HEAVY INDUSTRIES, LTD.
5-1, Marunouchi 2-chome, Chiyoda-ku, Tokyo, Japan
Cable Address: HISHIJU TOKYO

Mitsubishi Heavy Industries America, Inc.
873 Supreme Drive, Bensenville, IL 60106 Phone; (312) 860-4220

Mitsubishi International Corporation
873 Supreme Drive, Bensenville, IL 60106 Phone: (312) 860-4222

CIRCLE A-8 ON READER REPLY CARD

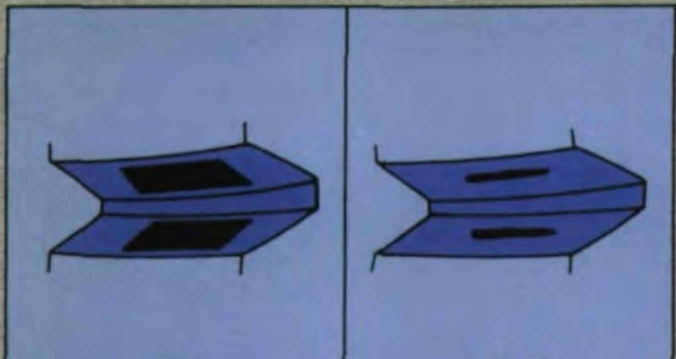

Fig. 6 Fig. 7

vex side of the gear tooth it runs from the flank at the toe to the top at the heel. On the concave side of the gear tooth the contact runs from the top at the toe to the flank at the heel.

Bias Out (Fig. 5)

The total offset value in the E & P check is less than the total pinion axial value.

A visual check of *bias out* can be made as follows:

The contact is diagonal to the pitch line, and on the convex side of the gear tooth it runs from the top at the toe to the flank at the heel. On the concave side of the gear tooth, the contact runs from the flank at the toe to the top at the heel.

Bias out is often required, in developing the tooth contact, due to the normal changes that take place during hardening, and to allow for the deflections in the mountings when the gears are in operation. A slight amount of *bias in* is desirable after lapping in automotive gears to give a quieter operating pair of gears. The line of contact as the tooth rolls into and out of engagement on the concave side of the pinion, starts in the flank at the heel and rolls out at the top at the toe, therefore, *bias in* increases the line of contact, but it will also decrease the amount of pinion mounting adjustment if the amount of *bias in* is too great.

Figs. 4 and 5 illustrate bias contacts. Regardless of the hand of spiral on the pinion, *bias in* will always run from the flank at the toe to the top at the heel on the convex side, and from the top at the toe to the flank at the heel on the concave side.

2. Profile Tooth Contact

The width of the contact (tooth profile) is as important as the length of the contact. A wide profile contact, Fig. 6, shows a contact covering the full depth of the tooth. Quite often there is a heavier concentration at the top of the tooth and in the flank of the tooth with the center of the tooth profile showing a lighter contact.

Too wide a profile contact is not desirable because even a slight amount of change in mounting distance would cause a definite concentration of load either high or deep on the tooth and may result in noisy gears which might also scuff or score along the area of concentration.

An extremely narrow profile contact, Fig. 7, shows a narrow concentration of contact in the center of the working depth. This condition permits a greater variation in mounting distance, but results in a noisier pair of gears which will also have a tendancy to scuff or score at the concentrated contact points.

In general, gears which have a wide profile before hardening will show a narrower profile after hardening. However, lapping will generally widen the profile, therefore an attempt should be made to obtain a profile width in cutting that will result in the hardened and lapped gears having a good profile adjustment and still be quiet in operation.

3. Interference Along Top Edge of Teeth

This condition is caused by an insufficient amount of backlash. It can be changed by adjusting the backlash when testing. Care must be taken not to decrease it too much because TOPREM interference will be introduced. Decreasing the backlash will also move the contact to the toe on both sides; on hypoid gears, it will cause the reverse side contact to be slightly lower on the gear (lameness) after testing.

4. Contact Too Long or Too Short on Either Side

This can be corrected by changing the cutter diameter on the pinion machine. When lapping, the value of the toe and heel swing cam settings or E & P settings should be increased on the side that is to be corrected for a long contact. To make a correction for a short contact the value should be decreased. (Fig. 8 & Fig. 9)

5. Crossed Contact

Changing the offset setting in the testing machine will cause the contact to move toward the toe on one side of the tooth and toward the heel on the opposite side. At the same time the contact will move high or deep on the tooth profile in

Fig. 8 – Long contact (full length) Fig. 9 – Short Contact

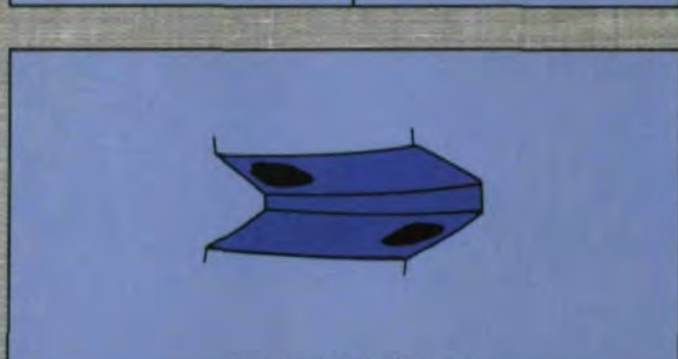

Fig. 10 – Crossed Contact

(continued on page 44)

VIEWPOINT

(continued from page 5)

Dear Editor:

As pointed out by a reader, the value of the helix angle in Table I of my article on helical gears in the March/April issue of GEAR TECHNOLOGY should have been 16.59467687. (helix angle = arc sin (π/11). This, incidentally was a misprint in the original publication in Machine Design.

Also, please note that I am enclosing Table 2 which was omitted.

Sincerely,
Eliot K. Buckingham, President
Buckingham Assoc., Inc.
Springfield, VT

Table 2 – Helix Angles for Exact Loads

Integer A	Helix Angle ψ_1	Integer A	Helix Angle ψ_1
4	51.75751851	15	12.08950814
5	38.92617544	16	11.32357080
6	31.57396132	17	10.64944699
7	26.66665193	18	10.05147839
8	23.12254873	19	9.51739193
9	20.43018899	20	9.03742809
10	18.31006687	21	8.60372642
11	16.59467687	22	8.20988341
12	15.17685827	23	7.85062891
13	13.98459310	24	7.52158526
14	12.96756767	25	7.21908557

Absorbing End Thrust Don't Make the Cure Worse than the Illness

All helical gears develop an end thrust that must be absorbed by a thrust bearing, angular contact roller bearing, or tapered roller bearing. If a thrust bearing is used and the gear shafts turn in plain journal bearings, then a free-body force analysis should be made in the gears to ensure that the gear blanks do not twist and that the shafts remain parallel. This analysis must include all external forces on the gear shafts and solidly connected elements.

To overcome the effects of end thrust, the double-helical (or herringbone) gear was developed. Here, the thrust from one helix supposedly balances the thrust from the other helix. However, even a single pair of helical gears is difficult to match, so double helicals (as in a herringbone drive) are virtually impossible to match. Usually, one gear (the pinion) is allowed to float and find its own center. But since this gear is moving axially, the loads on the helixes cannot be equal.

In a high speed set, the mass of the floating gear often prevents it from positioning, and one helix absorbs the full load. This bad situation is further compounded by the frequent use of high helix angles to increase the number of teeth in contact. But this alteration does not necessarily increase load carrying capacity.

the case of spiral bevel or hypoid gears. The movement will follow along the tooth in the *bias out* direction. (Fig. 10)

6. Incorrect Shaft Angle

The tooth contact on both sides of the tooth will be concentrated at the same end of the tooth. If the contact is concentrated at the toe the shaft angle is too large. If the contact is concentrated at the heel, the shaft angle is too small. It will be necessary in either case to correct the shaft angle to obtain the proper tooth contact. (Fig. 11, Fig. 12)

7. Incorrect Pinion Mounting Distance

Changing the pinion mounting (axial) distance will cause the contact to move high or deep on the tooth profile. See Figs. 13 and 14. Increasing the pinion mounting distance will move the contact toward the flank of the pinion and high on the gear. In the case of spiral bevel, or hypoid gears, the contact may also move toward the heel or toe.

8. Desired Tooth Contact

A localized tooth contact is desirable because it allows for displacement of the gear under operating loads without causing concentration of the load at the ends of the teeth. It also permits some variation in the final mountings without effecting the running qualities.

Fig. 15 shows a central toe contact. The contact extends along approximately one-half the tooth length and is nearer the toe of the tooth than the heel. The contact is also relieved slightly along the top and flank of the tooth. Under light loads the contact should be in this position on the tooth.

Fig. 16 shows the same tooth with a contact as it should be under full load. It should show slight relief at the ends and along the top and flank of the teeth with no load concentration at the extreme edges of the tooth.

A. Runout

Runout is characterized by a periodic variation in sound during each revolution and by the tooth contact shifting progressively around the gear from heel to toe and toe to heel.

B. Tooth Spacing

Tooth spacing error is a cumulative error which can build up around the gear, often causing a large error between the first and last tooth cut. These are known as tooth defects and are indicated by a knocking sound or a light or heavy tooth contact on one or more teeth.

Error in spacing and concentricity usually is the result of faulty arbor equipment, improper chucking or inaccurate gear blanks. These items should be checked before any changes are made on the cutting machine.

C. Noise

A poor finish usually results in vibration and increased noise when the gears are run together. A visual check will show a rough or uneven tooth contact. A poor finish is usually due to improper normalizing of the steel or to a steel of poor machinability. Poor finish can also result from improper cutting speeds or from dull cutters.

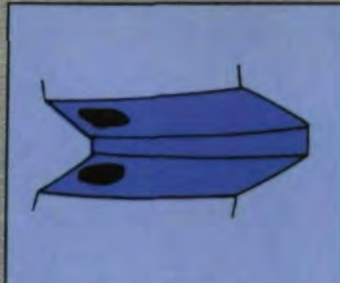

Fig. 11 – Toe Contact

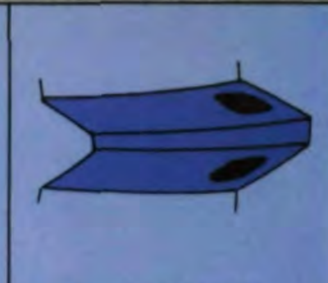

Fig. 12 – Heel Contact

Poor finish should not be confused with interferences, which will also give a rough finish and noisy operation. Visual observation will show interference as a heavy tooth contact along the top edge of the teeth on one member and in the flank of the teeth on the mating member.

Interference is usually a result of one of the following conditions:

1. Teeth cut too shallow.
2. Blanks machined incorrectly.
3. Fillet radius too large.
4. Tooth profile not completely generated (insufficient generating roll on the cutting machine).

General Testing Information

Increasing the offset (E+) will move the contact in the *bias out* direction on all spiral bevel or hypoid gears regardless of the hand of the spiral.

Decreasing the offset (E−) in relation to the pinion will move the contact toward the heel on the bottom side and toward the toe on the top side.

Fig. 13 – Flank Contact

Fig. 14 – Top Contact

Fig. 15

Fig. 16
Desired Contact Under Full Load

Decreasing the pinion axial distance (P−) will move the contact higher on the pinion tooth and lower on the gear tooth.

Swing movement in the lapping machine will move the contact along the tooth from toe to heel in the *bias out* direction, the same as the offset movement in the E & P check.

Counter-clockwise swing movement in the lapping machine will move the contact toward the heel on either side; clockwise swing movement will move the contact toward the toe on either side.

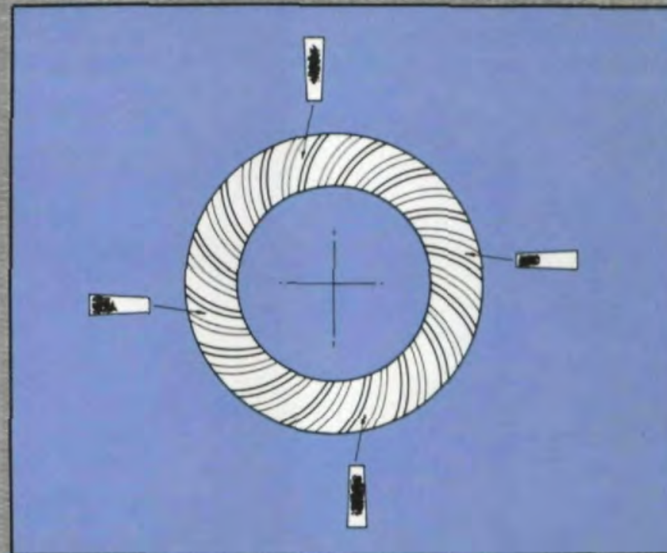

Fig. 17—Shifting of tooth contact shows presence of runout. Sound variation also characterizes the existence of runout.

Test Machine Adjustments and Their Effect on Tooth Contacts for Bevel Gears

Movements of the offset and pinion axial settings will move the tooth contact in the direction indicated in the following illustrations.

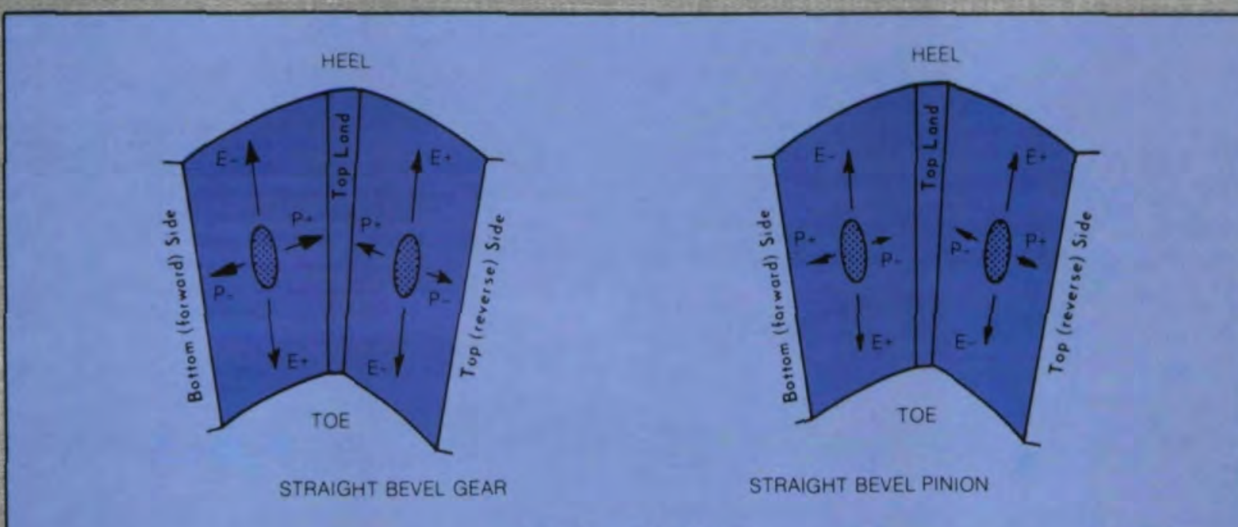

Straight Bevel Gears

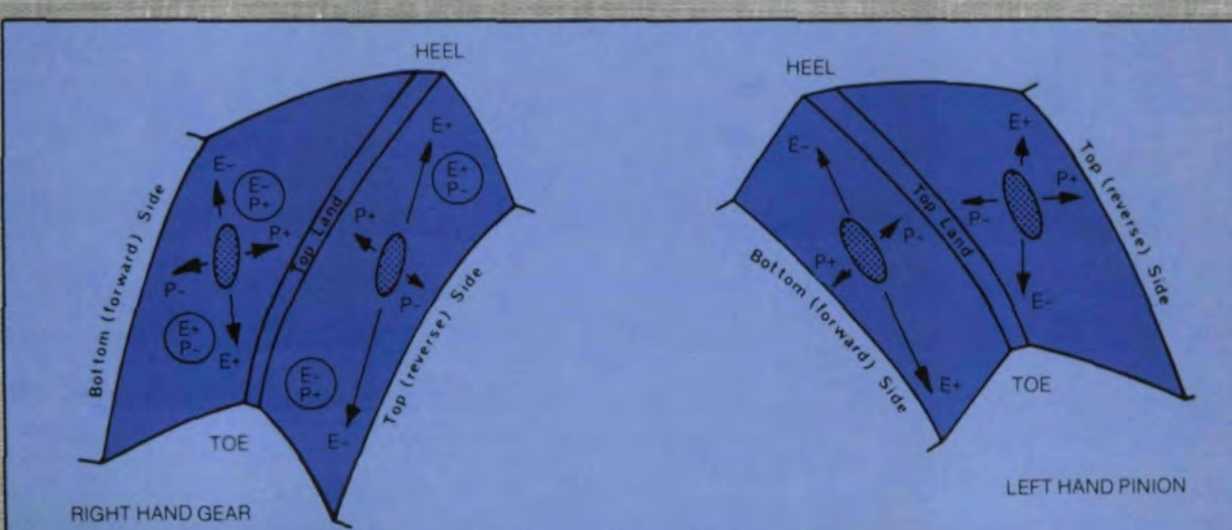

Left Hand Spiral Bevel Gears

(continued on page 46)

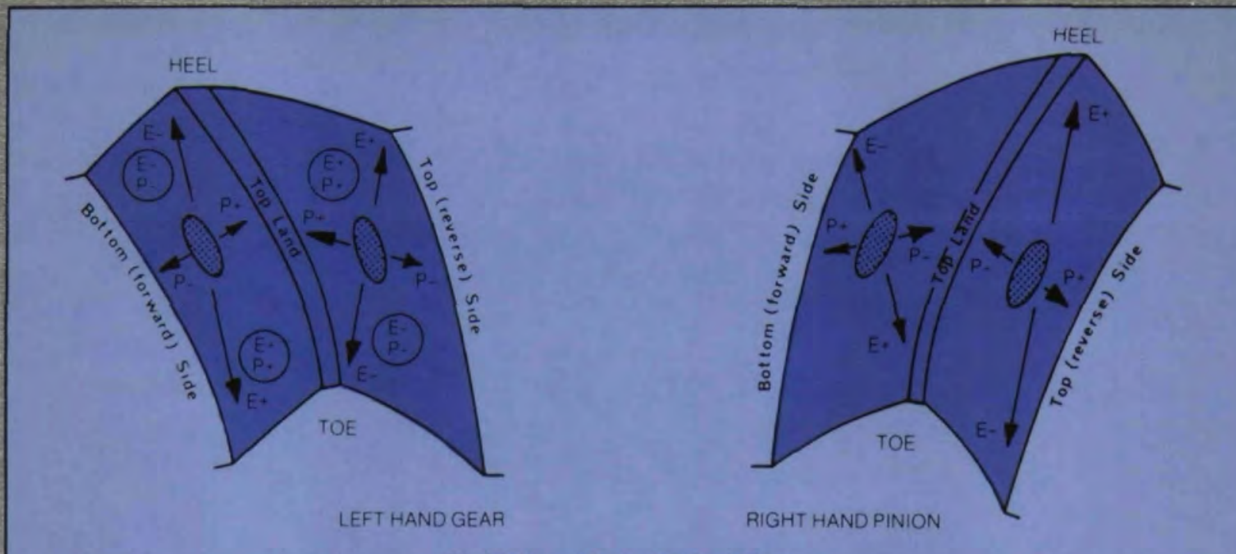

Right Hand Spiral Bevel Gears

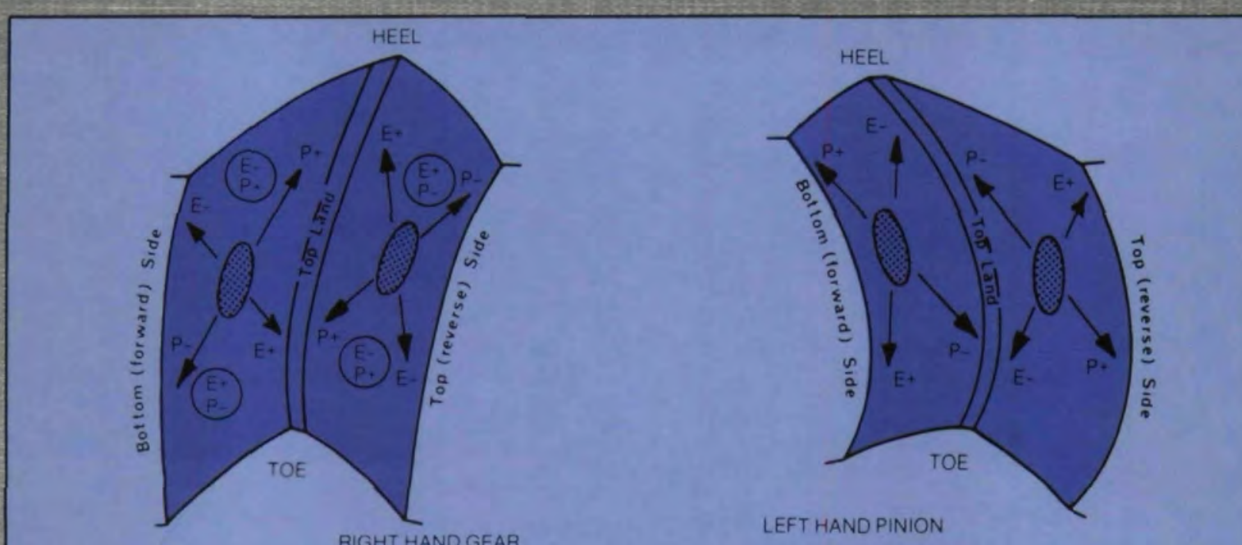

Left Hand Hypoid Gears

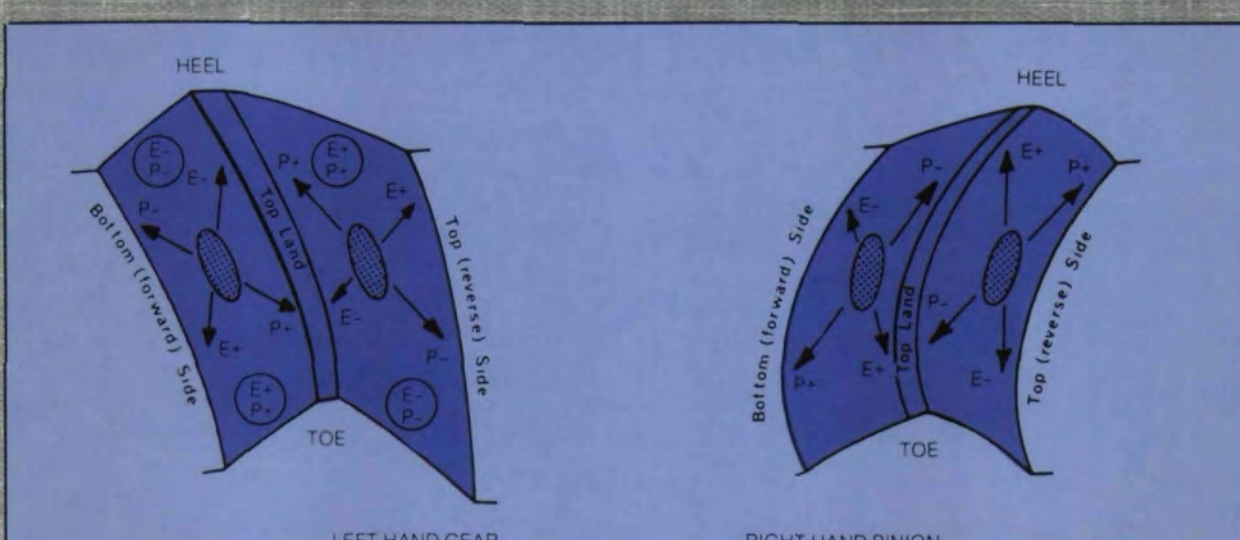

Right Hand Hypoid Gears

CLASSIFIED

Rates: Classified Display—$100 per inch (minimum 3") Type will be set to advertiser's layout or *Gear Technology* will set type at no extra charge. **Word Count:** 35 characters per line, 7 lines per inch.

Payment: Full payment must accompany classified ads. Mail copy to *Gear Technology,* P.O. Box 1426, Elk Grove Village, IL 60007. **Agency Commission:** No agency commission on classifieds.

Closing date: Ads must be received by the 25th of the month, two months prior to publication. **Acceptance:** Publisher reserves the right to accept or reject classified advertisements at his discretion.

SUBCONTRACT WORK

...and now **METRIC!**

GEAR TOOTH PITCH TEMPLATES

A VITAL NEW TOOL FOR SALESMEN & ENGINEERS

You can now make quick accurate metric gear tooth pitch identification with this handy new template set.

- Each template has been made to generated machine-cut accuracy from anodized aluminum for long life and corrosion resistance.
- The complete set includes 14½° and 20° pressure angles of the following module pitches: 1, 1½, 2, 2½, 3, 3½, 4, 4½, 5, 5½, 6, 7, and 8. The set of 19 templates identifies a total of 26 pitches and pressure angles. The templates are sold in sets only and include a carrying case.

GETTY ENTERPRISES
1843 Acorn Lane • Abington, PA 19001

CIRCLE A-18 ON READER REPLY CARD

HOBBER REBUILDING SPECIALISTS

Having trouble meeting today's demand quality control tolerances?

Let our factory trained and experienced staff return your machine to optimum operating condition.

We specialize in repairing, rebuilding and modernizing all makes of hobbers.

- Cleveland Rigidhobbers
- Gould & Eberhardt
- Barber Colman

PRESSMATION INC.
522 Cottage Grove Road
Bloomfield, Conn. 06002
(203) 242-8525

CIRCLE A-24 ON READER REPLY CARD

There's still time...
closing date for a classified ad in the Sept./Oct. issue is **July 20.**

GEAR DESIGN WITH YOUR PERSONAL COMPUTER

Enjoy convenience and time savings by using your personal computer for gear design. Reduce gear design from 3-4 hours to under 30 minutes!!!

Gear redesign is easy . . . recall previous design from the electronic library; change *just the revised factors* and you're finished . . . complete with a record of the design specifications and a *gear profile drawing!!!!*

Programs satisfy most external helical or spur gear specifications for . . .

- Standard or non-standard gears.
- Various gear material properties.
- Gear size or gear ratios.
- Bending/surface stresses with varying load/speed conditions.
- Contact ratio calculates potential for *meshing interference.*

ENGINEERING SOFTWARE COMPANY
Three Northpark East, Suite 901
8800 North Central Expressway, Dallas, TX 75231
(214) 361-2431

CIRCLE A-21 ON READER REPLY CARD

GEAR TOOTH GRINDING & HONING ONLY

Production Quantities
3/4" P.D. to 27.5" P.D.;
3.5 D.P. and 11" Face

We have no turning, hobbing or shaping capability

ALLEGHENY GEAR CORP.
23 Dick Road
Depew, NY 14043
716-684-3811

CIRCLE A-17 ON READER REPLY CARD

FOREST CITY GEAR invites you to visit our plant which features the most modern gear hobbing machines in the world.

We cut gears to 16" in diameter and 36" in length. Cutting ultra precision gears in high volume is our specialty. Crown hobbing to reduce gear noise on auto-loading hobbers puts us in a class by ourselves.

See our latest CNC Koepfer 173 gear machine at IMTS McCormick, North Level 2 at Cosa booth #6243.

FOREST CITY GEAR
11715 Main Street
Roscoe, IL 61073
(815) 623-2168

CIRCLE A-22 ON READER REPLY CARD

HELP WANTED

GEAR PERSONNEL

ENGINEERS
GEAR GRINDERS
MACHINISTS
PRODUCTION CONTROL
QUALITY CONTROL/INSPECTION
SALES
SHOP SUPERVISION, ETC.

If you are in the gear business in any capacity, are ambitious and thinking of making a move, send us your resume. The above and other new positions are being created by internal growth at both our San Diego, California & Roseville, Michigan plants.

ACR INDUSTRIES, INC.
29200 Calahan
Roseville, Michigan 48066

Bring in new customers for your business by advertising in GEAR TECHNOLOGY, The Journal of Gear Manufacturing.

Call (312) 437-6604

MECHANICAL EFFICIENCY OF DIFFERENTIAL GEARING . . .
(continued from page 16)

no friction loss certainly does not coincide with reality, and in some cases the analytical results with this assumption will lead to wrong conclusions. The method introduced in this article for analyzing efficiency is simple, explicit, and applicable to all differentials with two degrees of freedom. Although the example given was an input-coupled system, the principles and formulas are equally applicable to output-coupled systems.

It has been pointed out that a "basic speed ratio," given the symbol R_o in this article, should be defined in a specific manner, so that it will express the significant characteristic features of the differential and be most useful for analysis and calculation.

The classification system of differential gearing used in this article is different from conventional systems such as that given in the *Gear Handbook*.[14] This classification is considered advantageous in emphasizing the significant differences of the various design possibilities.

The great number of design possibilities inherent in the use of differential gearing has been pointed out, especially if designs are employed that allow the basic members to interchange positions over the range of operation. Computer-aided design can be of significant help in developing an optimum design from the numerous possibilities. A flow chart and summary of an applicable computer program have been presented.

References

1. BEACHLEY, N. H., et al., "Continuously-Variable Transmission Designs for Flywheel-Hybrid Automobiles," *Proceedings of the International Symposium on Gearing and Power Transmissions,* Tokyo, 1981, pp. 393-398.
2. WHITE, G., "Properties of Differential Transmissions," *The Engineer,* Technical Contribution Section, July 28, 1967, pp. 105-111.
3. WHITE, G., "A Two-Path Variable-Ratio Transmission with an Extended Range of Ratios," ASME *Journal of Engineering for Industry,* Aug. 1977, pp. 656-661.
4. WHITE, G., "Compounded Two-Path Variable Ratio Transmissions With Coaxial Gear Trains," *Mechanism and Machine Theory,* Vol. 11, 1976, pp. 227-240.
5. MACMILLAN, R. H., and DAVIES, P. B., "Analytical Study of Systems for Bifurcated Power Transmission," *Journal of Mechanical Engineering Science,* Vol. 7, No. 1, 1965, pp 40-47.
6. STUBBS, P. W. R., "The Development of a Perbury Traction Transmission for Motor Car Applications," ASME paper 80-C2/DET-59, 1980.
7. KUDLYAVTZEV, V. H., *Planetary Gearing* (Russian) Machine-Building Publisher, 1966.
8. YU, DAVID, "Problems Arising in the Calculation of Gearing Efficiency," *Liaoning Machine* (Chinese), No. 2, 1980, pp. 33-42.
9. MACMILLAN, R. H., "Epicylic Gear Efficiencies," *The Engineer,* Dec. 23, 1949, pp. 727-728.
10. MACMILLAN, R. H., "Power Flow and Loss in Differential Mechanisms," *Journal of Mechanical Engineering Science,* Vol. 3, No. 1, 1961, pp. 37-41.
11. MOROZUMI MUNEHARU, "The Efficiency and the Design of Modified Internal Gearing," *Mechanical Researches* (Japanese), No. 5, 1970, pp. 720-726.
12. YU, DAVID, "The Optimizing Programming Design of the KHV Planetary Gear Driving," *Proceedings of the International Symposium on Gearing and Power Transmissions,* Tokyo, 1981, pp. 295-299.
13. YU, DAVID, and BEACHLEY, N. H., "Alternative Split-Path Traction Drive Transmission Designs for Motor Vehicle Application," *Proceedings, First International Symposium on Design and Synthesis,* Tokyo, July 1984.
14. DUDLEY, D. W., et al., *Gear Handbook,* McGraw-Hill, New York, 1962.

This article was previously presented at the ASME Design Engineering Technical Conference, October 1984. Paper No. 84-Det-102.

Fig. 14—Fraction of power through the CVU for zero friction loss

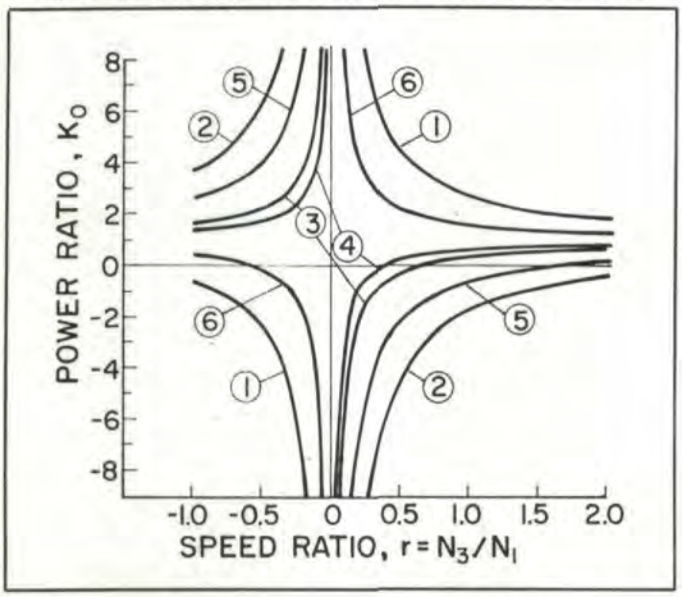

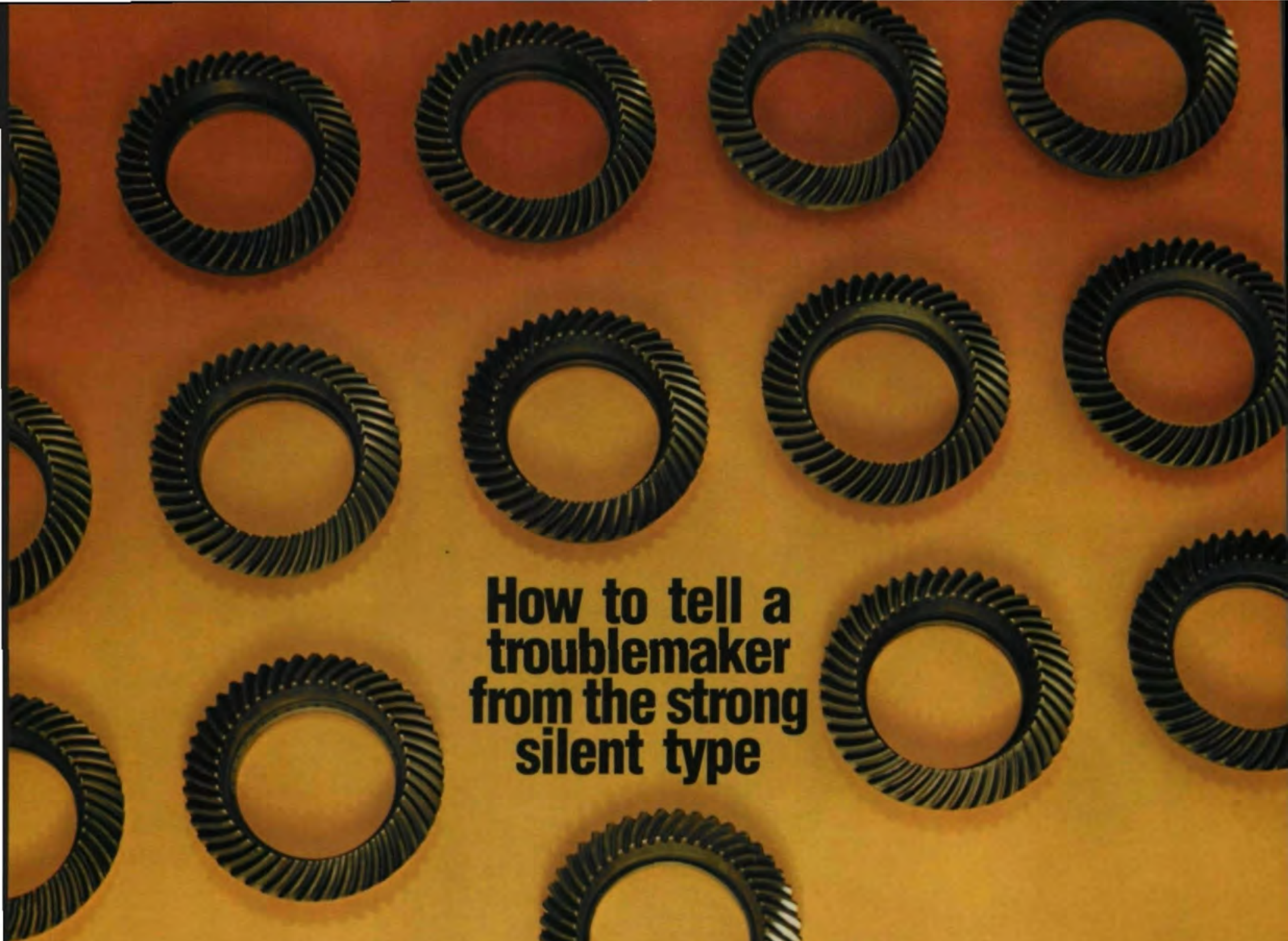

How to tell a troublemaker from the strong silent type

With G-AGE™, the complete line of gear testing and measurement equipment and programs

Some of the nicest looking gears start whining and grumbling as soon as they're put to work. And that's one kind of trouble you want to stop before it starts. You can — easily and efficiently — with G-AGE test and measurement products from Gleason.

G-AGE is the most complete gear-inspection line of its kind in the world. If you make or use bevel, hypoid, or helical gears, there's a G-AGE product for you. One that will tell you exactly what you need to know for effective QA/QC at incoming inspection or at any stage in gear manufacturing.

The G-AGE line includes:

- Rolling contact checkers for your expert inspectors.
- A full range of elemental testers to check tooth position and geometry or shape.
- Programs for coordinate measuring to determine tooth form errors based on design data and to provide corrective machine settings.
- Sophisticated single-flank testing systems that let you investigate transmission error and most related parameters of a gear or gear pair.
- The ultimate gear QC system — the 579 Automatic Data Analysis System. Interfaced with any G-AGE single-flank tester, it automatically interprets test data to give you more answers, in more usable form, than any other system.

G-AGE is your key to higher quality gears, less scrap, lower costs, and a greater degree of control than ever before possible.

Nobody knows more about gears and gear testing than Gleason. Let us help you select the G-AGE equipment or program you need to eliminate potential troublemakers before they can start a rumble. Call 716-473-1000 or write Gleason Works, 1000 University Avenue, Rochester, NY 14692, U.S.A

GLEASON

Advanced concepts, traditional quality. That's the new Gleason.

Visit Gleason Booth #6333 at IMTS '86

CIRCLE A-20 ON READER REPLY CARD